AGU100 ADVANCING EARTH AND SPACE SCIENCE

JGR Biogeosciences

RESEARCH ARTICLE
10.1029/2018JG004701

Key Points:
- pCO_2, pCH_4, and CO_2 fluxes in floodplain ponds varied on a diel basis with in situ respiration
- pCH_4 and CH_4 fluxes varied seasonally, from reservoir drawdown to floodplain inundation
- Floodplains during reservoir drawdown can be nontrivial sources for diffusive CH_4 to the atmosphere

Supporting Information:
- Supporting Information S1
- Figure S1
- Figure S2

Correspondence to:
B. L. Miller,
blmiller3@gmail.com

Citation:
Miller, B. L., Chen, H., He, Y., Yuan, X., & Holtgrieve, G. W. (2019). Magnitudes and drivers of greenhouse gas fluxes in floodplain ponds during drawdown and inundation by the Three Gorges Reservoir. *Journal of Geophysical Research: Biogeosciences*, *124*, 2499–2517. https://doi.org/10.1029/2018JG004701

Received 16 JUL 2018
Accepted 4 JUL 2019
Accepted article online 18 JUL 2019
Published online 13 AUG 2019
Corrected 13 SEP 2019

This article was corrected on 13 SEP 2019. See the end of the full text for details.

Author Contributions:
Conceptualization: B. L. Miller, H. Chen, Y. He, X. Yuan, G. W. Holtgrieve
Data curation: B. L. Miller, H. Chen, Y. He
Formal analysis: B. L. Miller
Funding acquisition: B. L. Miller, H. Chen, G. W. Holtgrieve
Investigation: B. L. Miller, Y. He
Methodology: B. L. Miller, H. Chen, Y. He, X. Yuan, G. W. Holtgrieve
Project administration: B. L. Miller, H. Chen, Y. He, X. Yuan
Visualization: B. L. Miller
Writing - original draft: B. L. Miller
(continued)

Magnitudes and Drivers of Greenhouse Gas Fluxes in Floodplain Ponds During Drawdown and Inundation by the Three Gorges Reservoir

B. L. Miller[1,2], H. Chen[1], Y. He[1], X. Yuan[3], and G. W. Holtgrieve[2]

[1]Chengdu Institute of Biology, Chinese Academy of Sciences, Chengdu, China, [2]School of Aquatic and Fishery Sciences, University of Washington, Seattle, WA, USA, [3]College of Resources and the Environment, Chongqing University, Chongqing, China

Abstract Hydropower reservoirs are well-known emitters of greenhouse gases to the atmosphere. This is due in part to seasonal water level fluctuations that transfer terrestrial C and N from floodplains to reservoirs. Partial pressures and fluxes of the greenhouse gases CH_4, CO_2, and N_2O are also a function of in situ biological C and N cycling and overall ecosystem metabolism, which varies on a diel basis within inland waters. Thus, greenhouse gas emissions in hydropower reservoirs likely vary over seasonal and diel time scales with local hydrology and ecosystem metabolism. China's Three Gorges Reservoir is among the largest and newest in the world, with a floodplain that encompasses approximately one third of the reservoir area. We measured diel partial pressures and fluxes of greenhouse gases in ponds on the Three Gorges Floodplain. We repeated these measurements on the submerged floodplain following inundation by the Three Gorges Reservoir. During reservoir drawdown, CH_4 ebullition comprised 60–68% of emissions from floodplain ponds to the atmosphere. Using linear mixed effects modeling, we show that partial pressures of CH_4 and CO_2 and diffusive CO_2 fluxes in floodplain ponds varied on a diel basis with in situ respiration. Floodplain inundation by the Three Gorges Reservoir significantly moderated areal CH_4 diffusion and ebullition. Diel pCO_2, pCH_4, pN_2O, and diffusive fluxes of CO_2 on the submerged floodplain were also driven by in situ respiration. The drawdown/inundation cycle of the Three Gorges Reservoir therefore changes the magnitudes of aquatic greenhouse gas fluxes on its floodplain.

Plain Language Summary Considered to be clean sources of energy, reservoirs emit greenhouse gases like other inland waters. Reservoir water levels fluctuate seasonally, introducing terrestrial organic matter to dammed rivers. Greenhouse gases such as methane and carbon dioxide are produced daily when organic matter is respired by aquatic microbes. This is balanced by consumption of carbon dioxide during daytime photosynthesis. We measured concentrations and fluxes of methane, carbon dioxide, and nitrous oxide over 24 hr in ponds on the Three Gorges Floodplain. We repeated these measurements in the overlaying Three Gorges Reservoir following its inundation of the floodplain. Among the different flux pathways, methane bubbles comprised the bulk of greenhouse gas emissions from floodplain ponds. Daily methane and carbon dioxide concentrations and carbon dioxide fluxes in these floodplain ponds varied with microbial respiration. By contrast, methane fluxes were much lower per unit area following floodplain inundation by the Three Gorges Reservoir. Daily concentrations of these gases and carbon dioxide fluxes were also driven by microbial respiration on the submerged floodplain. Seasonal water level fluctuations in the Three Gorges Reservoir therefore change how greenhouse gases move to the atmosphere on its floodplain.

1. Introduction

Impounded rivers are an important component of the global carbon (C) cycle, contributing 4–17% of C emitted from inland waters to the atmosphere each year (Aufdenkampe et al., 2011; Barros et al., 2011; Deemer et al., 2016). A recent synthesis of hydropower reservoirs measured globally found that 84% were sources for diffusive carbon dioxide (CO_2), and all were either sources for diffusive methane (CH_4) or CH_4 neutral (Deemer et al., 2016). Hydropower reservoirs occur in larger watersheds than naturally occurring lakes and receive comparatively high nutrient and organic matter (OM) inputs, which influence in situ primary production and respiration (Hayes et al., 2017; Knoll et al., 2003; Mendonca et al., 2017). Reservoirs also receive OM through the flooding of terrestrial landscapes during reservoir formation and subsequent

Writing – review & editing: B. L. Miller, H. Chen, G. W. Holtgrieve

fluctuations in water storage (Jacinthe et al., 2012; Maeck et al., 2014). Growth of terrestrial OM on reservoir floodplains is transferred to reservoirs during often predictable seasonal drawdown/inundation cycles (Junk et al., 1989; Battin et al., 2008; Chen, Wu, et al., 2009; Chen, Yuan, et al., 2009). Respiration of terrestrial OM proceeds considerably faster in lakes, rivers, and flooded soils (Battin et al., 2008; McNicol & Silver, 2014). Riverine OM concentrations have been shown to spike following inundation of subtropical and temperate floodplains (Burns & Ryder, 2001; Vasquez et al., 2015; Wainright et al., 1992). This likely results in concurrent spikes in diffusive CH_4 and CO_2 emissions as OM is respired.

Bubbling or ebullition is another important pathway for CH_4 to the atmosphere in temperate (Del Sontro et al., 2010) and tropical (Del Sontro et al., 2011) reservoirs. Sparingly soluble CH_4 may be produced in anaerobic sediments more quickly than sediment-water diffusion rates and form bubbles (Fendinger et al., 1992; Mattson & Likens, 1990). These bubbles rise to the water's surface, undergoing minimal oxidation (Del Sontro et al., 2010; Ostrovsky et al., 2008). Deemer et al. (2016) estimate that ebullition comprises an average of 65% of total CH_4 emissions from reservoirs globally. Under low and dynamic hydrostatic pressures on submerged floodplains, ebullition is likely a key component of CH_4 emissions.

There have been fewer measurements of N_2O emissions from hydropower reservoirs. The recent synthesis by Deemer et al. (2016) included flux measurements from 161 reservoirs for CH_4, 229 for CO_2, and just 58 for N_2O. Tropical (Guerin et al., 2008; Naqvi et al., 2018), subtropical (Chen, Yuan, et al., 2009; Yuan, et al., 2009; Li et al., 2018; Zhao et al., 2013; Zhu et al., 2013), temperate (Beaulieu et al., 2014; Deemer et al., 2011; Li et al., 2018; Tomaszek & Czerwieniec, 2003), and boreal (Huttunen et al., 2002) reservoirs that have been measured indicate that they are also sources for N_2O. N_2O has 298 times the global warming potential of CO_2 on a per molar basis in the atmosphere over a 100-year time scale, making it an important addition to measurements of reservoir greenhouse gas emissions (IPCC, 2001; Myhre et al., 2013).

CH_4, CO_2, and N_2O within inland waters result from metabolic fixation and respiration of C and nitrogen (N). Most studies of hydropower reservoirs and other aquatic ecosystems concentrate sampling at a single point during the day, despite this association with ecosystem metabolism. Odum (1956) classically showed the metabolic balance of inland waters to be more autotrophic during the day and more heterotrophic during the night using net oxygen (O_2) dynamics. Tobias et al. (2007), Hotchkiss and Hall (2014), and Schindler et al. (2017) have since shown that daytime aerobic respiration can be 54–340% of nighttime respiration in temperate lakes and streams. They attribute this to greater production of labile OM algal exudates (Bains & Pace, 1991; Cole et al., 1982; Kaplan & Blott, 1982) and higher temperatures during the day (Yvon-Durocher et al., 2012). Decoupling of CO_2 partial pressures from O_2 dynamics and correlations to primary production and aerobic respiration have also been shown by others (Peeters et al., 2016; Stets et al., 2017). Thus, metabolic properties such as dissolved O_2 and temperature have the potential to influence net consumption or production of CO_2 differently over 24 hr. How the partial pressures and fluxes of CH_4 and N_2O vary with ecosystem metabolism on diel time scales is less clear (Hoellein et al., 2013).

Efforts have been made to characterize greenhouse gas emissions from hydropower at other temporal and spatial scales. Hydropower reservoirs less than 10–20 years old tend to emit more CH_4 and CO_2 per unit area than older hydropower reservoirs (Barros et al., 2011; St. Louis et al., 2000). Of these, reservoirs in tropical regions tend to emit more CH_4 and CO_2 per unit area than reservoirs in temperate regions (Barros et al., 2011; Galy-Lacaux et al., 1997). Current rates of hydropower development are greatest in tropical and subtropical regions (Zarfl et al., 2015). Some of the highest rates of impoundment (>100 dams currently planned) are in China's Yangtze River basin (Zarfl et al., 2015), making these newly constructed, subtropical reservoirs likely greenhouse gas emitters.

The Three Gorges Reservoir on the Yangtze River represents an opportunity for the study of diel greenhouse gas emissions from a comparatively new subtropical hydropower reservoir and its floodplain. Filled in 2010, the Three Gorges Reservoir is among the largest in the world, covering 1,106 km^2 in central China (Zhang et al., 2018). The Three Gorges Floodplain covers 321 km^2 or just under one third of the reservoir's area (Zhang et al., 2018). Studies by Chen, Wu, et al. (2009), Chen, Yuan, et al. (2009), Zhao et al. (2013), Zhu et al. (2013), Li et al. (2013), and Zhou et al. (2017) have quantified diffusive CH_4, CO_2, and N_2O fluxes in the region. However, none have measured diel fluxes and CH_4 ebullition during both reservoir drawdown and inundation on the Three Gorges Floodplain.

The Three Gorges Floodplain is increasingly targeted by displaced farmers for pond aquaculture in attempts to supplement agricultural productivity during reservoir drawdown (Li et al., 2013; Zhang et al., 2018; Zhou et al., 2017). Globally, ponds less than 1,000 m^2 are hot spots for CH_4 and CO_2 emissions (Holgerson & Raymond, 2016). Although water bodies this size are difficult to detect and delineate from wetlands using satellite imagery, it is thought that ponds comprise approximately 9% of nonrunning or lentic inland waters, which include lakes and reservoirs (Holgerson & Raymond, 2016). Holgerson and Raymond (2016) estimate that natural ponds contribute 40% of diffusive CH_4 emissions from lentic inland waters worldwide. Ponds created on the terrestrial landscape for a variety of purposes including stock watering, irrigation, and aquaculture have been also found to emit CH_4 (Ollivier et al., 2019; Peacock et al., 2019). In some cases, these ponds emit CH_4 at higher rates than natural ponds through diffusive and ebullition flux pathways (Grinham et al., 2018), though more comparative data are needed. Natural and aquaculture ponds are among the aquatic environments that remain on the Three Gorges Floodplain during approximately 6 months of reservoir drawdown, from April to September each year. These expanding environments on the Three Gorges Floodplain are likely emissions hot spots.

In this study, we measured diel greenhouse gas partial pressures and fluxes during both reservoir drawdown and inundation on the Three Gorges Floodplain. During reservoir drawdown, we carried out measurements in a natural pond and a newly created aquaculture pond. We repeated these measurements on the submerged floodplain following inundation by the Three Gorges Reservoir. We used linear mixed effects modeling to determine relative importance of ecosystem metabolism to observed diel patterns of CH_4, CO_2, and N_2O partial pressures and diffusive fluxes. By conducting field-based measurements of C and N cycling, we account for commonly overlooked contributions of CH_4 emissions from floodplain ponds. We show that greenhouse gas partial pressures and fluxes vary over both seasonal and diel time scales along with drawdown/inundation cycle and ecosystem metabolism.

2. Materials and Methods

2.1. Study Sites

We conducted this study in the Pengxi River Wetland Reserve on the Three Gorges Floodplain between June 2014 and January 2015 (Figure 1). This region of P.R. China is characterized by a subtropical, humid monsoonal climate, with a mean annual temperature of 18.2 °C and a mean annual precipitation of 1,200 mm. The Pengxi River Wetland Reserve occupies 36.9 km^2 at elevations ranging from 160 to 175 m above sea level (a.s.l.). During reservoir drawdown, water levels in the Three Gorges Reservoir are 145 m a.s.l., leaving much of the reserve exposed at preimpoundment levels (Figure 1b). We sampled one natural pond (31°5′37.74″ N, 108°27′45.05″ E, 150 m a.s.l., 488-m^2 area, 54-cm mean depth) and one aquaculture pond (31°12′30.26″ N, 108°27′0.05″ E, 159 m a.s.l., 314-m^2 area, 82-cm mean depth). The aquaculture pond was used to cultivate the emergent macrophyte *Nelumbo nucifera* (lotus). Water storage in the Three Gorges Reservoir increases to 175 m a.s.l. from September to February, submerging most of the reserve (Zhou et al., 2017; Figure 1c). We repeated sampling at the same study sites on the submerged floodplain following inundation by the Three Gorges Reservoir.

2.2. Partial Pressures

We sampled three replicate partial pressures of CH_4, CO_2, and N_2O from a water depth of 10 cm in the natural and aquaculture ponds every 12 hr, for 24 hr, on 28–29 June, 9–10 August during a rain event (12-mm rain), and 13–14 August after a rain event (reservoir drawdown). We sampled three replicate partial pressures every 2 hr, for 24 hr, at the same study sites after they were submerged by the Three Gorges Reservoir on 4–5 January. Along with each of these partial pressures in water, we sampled three replicate partial pressures in ambient air 1 m above the water's surface. Water samples were equilibrated following Kling et al. (2000). Equilibrated water samples and ambient air samples were stored in evacuated 5-ml glass vials and analyzed using gas chromatography in the College of Forestry at Northwest Agricultural and Forestry University in Xi'an, P.R. China (PE Clarus 500, PerkinsElmer, Inc., USA, equipped with a flame ionizer detector operating at 350 °C and a 2-m Porapak 80–100 Q Column).

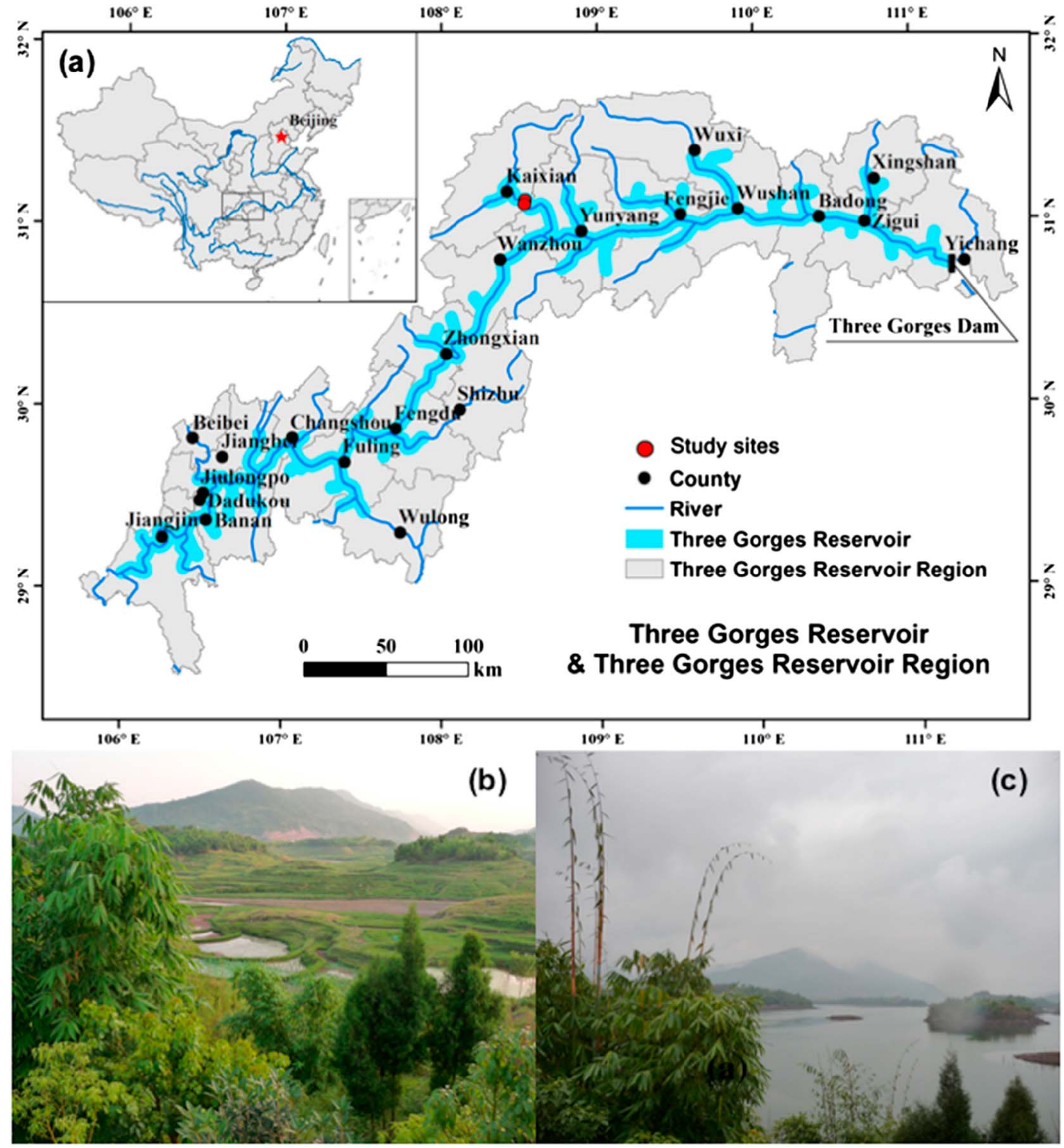

Figure 1. Three Gorges Reservoir on the Yangtze River and its tributaries, with study sites in the Pengxi River Wetland Reserve (a). Blue shading represents the extent of the reservoir during peak floodplain inundation. Study sites were one natural pond and one aquaculture pond on the Three Gorges Floodplain during reservoir drawdown (b) and on the submerged floodplain following inundation by the Three Gorges Reservoir (c).

2.3. Diffusive Fluxes

We sampled diffusive CH_4, CO_2, and N_2O fluxes in the natural and aquaculture ponds every 2 hr, for 24 hr, during the June, August, and January sampling events using three replicate floating chambers (Keller & Stallard, 1994). Chambers measured 29.5-cm height above the surface of the water by 31.5-cm width by 31.5-cm depth and were made of heat-insulated propathene plastic. Headspace from each chamber was collected at 0, 5, 10, and 15 min following enclosure and stored in evacuated 5-ml glass vials. All samples were analyzed as above. Diffusive fluxes were determined following Frankignoulle (1988) and Alin et al. (2011):

$$F_{\mathrm{D}} = \left(\frac{\mathrm{d}P}{\mathrm{d}t}\right)\left(\frac{V}{RT_{\mathrm{K}}A}\right), \tag{1}$$

where F_{D} is diffusive flux (mg CH_4, CO_2, or N_2O m^2/hr; mg·m^{-2}·day^{-1}) measured directly using floating

10.1029/2018JG004701

chambers, P is the partial pressure of CH_4, CO_2, or N_2O (uatm), t is time (min), V is the volume of the floating chamber (L), R is the ideal gas constant (L atm·mol^{-1}·K^{-1}), T_K is air temperature in degrees Kelvin, and A is the surface area of the floating chamber (m^2; $n = 973$ total). Each diffusive flux therefore results from a linear regression of four partial pressures that increase or decrease over time. For a positive diffusive flux, the regression is

$$y_i = \beta_1 x_1 + \beta_2 x_2 + \beta_3 x_3 + \beta_4 x_4, \tag{2}$$

where y_i is any observed partial pressure of CH_4, CO_2, or N_2O; $\beta_{1\ldots4}$ are the regression coefficients; and $x_{1\ldots4}$ are 0, 5, 10, and 15 min. Highly influential data points or outliers in this linear regression resulting from measurement and experimental errors were identified using the difference between the fitted value and the difference in betas (Kutner et al., 2004). The difference between the fitted value was determined using

$$DFFIT = \frac{\hat{y}_i - \hat{y}_{i(i)}}{\sqrt{MSE_{(i)} h_{ii}}}, \tag{3}$$

where $DFFIT$ is the difference between the fitted value, $\hat{y}$ is the estimate of y_i using all data points, $y_{i(i)}$ is the estimate of y_i using the regression model with the ith observation omitted, MSE_i is the mean square error for the regression model with the ith observation omitted, and h_{ii} is the ith diagonal term for the hierarchical matrix using all values. The difference between betas was determined using

$$DFBETAS = \frac{\hat{\beta}_k - \hat{\beta}_{k(i)}}{\sqrt{MSE_{(i)} c_{kk}}}, \tag{4}$$

where $DFBETAS$ is the difference between betas, $\hat{\beta}_k$ is the regression coefficient for the kth parameter using all data points, $\hat{\beta}_{k(i)}$ is the regression coefficient for the kth parameter with the ith observation omitted, and c_{kk} is the kth diagonal element in the matrix $(X'X)^{-1}$. Thresholds of $|DFFIT| > 2$ and $|DFBETAS| > 2$ were set for omission of highly influential positive and negative data points in regression models. Such omissions typically moderated diffusive fluxes.

2.4. Ebullition

We estimated CH_4 ebullition (mg·m^{-2}·hr^{-1}) in shallow water (<2 m) using the distribution and variance in gas transfer velocities among the four replicate floating chambers during the June, August, and January sampling events. Essentially, if one chamber's apparent gas transfer velocity was substantially larger than those measured in adjacent chambers, we assumed that it received ebullition. The apparent gas transfer velocity at ambient temperature in centimeters per hour, k_T, was calculated following Bastviken et al. (2004, 2010) and Sawakuchi et al. (2014):

$$k_T = \left(\frac{\mathrm{d}P}{\mathrm{d}t}\right) \frac{V\,(P_w - P_0)}{K_H\, R T_K A}, \tag{5}$$

where P is the partial pressure of CH_4 (μatm), t is time (min), V is the volume of the floating chamber (L), P_w is the partial pressure of CH_4 inside the chamber in equilibrium with P_{aq} (μatm), P_0 is the partial pressure of CH_4 inside the chamber at $t = 0$ (μatm; presumably local atmospheric), K_H is the temperature-dependent Henry's constant (mmol·L^{-1}·atm^{-1}; Figure 3) (Wilhelm et al., 1977), R is the ideal gas constant (L atm·-mol^{-1}·K^{-1}), T_K is water temperature in degrees Kelvin, and A is the surface area of the floating chamber (m^2). The Schmidt number (Sc) for kinematic viscosity and the gas transfer velocity given a Sc of 600, k_{600}, were also calculated following Wanninkhof (1992):

$$Sc = 1897.8 - (114.28\, T_K) + \left(3.2902\, {T_K}^2\right) - \left(0.039061\, {T_K}^3\right), \tag{6}$$

$$k_{600} = k_T \left(\frac{600}{Sc}\right)^{-0.5}. \tag{7}$$

Ratios were then created for calculated k_{600}:minimum k_{600} in each of the four replicate floating chambers. Because there were two clear groups in binned ratios for <6.5 and >6.5, chambers with a ratio >6.5 were

10.1029/2018JG004701

assumed to have received ebullition (supporting information Figure S1). Diffusive CH_4 flux was calculated using the minimum k_{600} from equations (6) and (7), and CH_4 ebullition was assumed to be the remaining flux.

We also sampled CH_4 ebullition ($mg \cdot m^{-2} \cdot day^{-1}$) in deep water (16–25 m) during the January sampling event using inverted funnels (n = 14). Funnels were made of vinyl with minimal seams and no openings along their interior collection surfaces. Funnels channeled CH_4 bubbles from a circular, 0.79-m^2 opening at a water depth of 2 m into a sealed syringe at their terminus (Environnement Illumite, Inc.; Strayer & Tiedje, 1978; Del Sontro et al., 2010). According to Ostrovsky et al. (2008), CH_4 bubbles collected at this depth in an unstratified water column undergo <5% oxidation before reaching the surface. We assumed that ebullition measured at this depth represented emissions from the water surface. Because ebullition can be a stochastic phenomenon, funnels were deployed continuously over 24 hr. Upon retrieval, headspace was sampled using a syringe, stored, and analyzed as described above. Ebullition was determined using

$$F_{\mathrm{E}} = \frac{(pCH_4K_H)V}{t_{\mathrm{d}}A_{\mathrm{f}}}, \tag{8}$$

where F_{E} is CH_4 ebullition ($mg \cdot m^{-2} \cdot day^{-1}$) in deep water, pCH_4 is the partial pressure of CH_4 inside of the collected bubbles (μatm), K_{H} is the temperature-dependent Henry's constant ($mmol \cdot L^{-1} \cdot atm^{-1}$), V is the bubble volume in the collection syringe (L), t_{d} is the deployment time (days), and A_{f} is the cross-sectional area of the sampling funnel (0.79 m^2).

2.5. Water Quality

We measured dissolved O_2 (mg/L), water temperature (°C), pH, and chlorophyll a (μg/L) from a water depth of 10 cm using a multiparameter sonde (YSI 6920, YSI, Inc., USA) every 2 hr, for 24 hr, during each diffusive flux measurement. Dissolved O_2 data were then used to calculate Apparent Oxygen Utilization (*AOU*) in milligrams per liter, or the departure from atmospheric equilibrium concentrations of O_2 due to utilization of this dissolved gas by aerobic respiration, following Richey et al. (1988):

$$AOU = pO_{2,eq}K_{\mathrm{H}} - [O_2]_{\mathrm{measured}}, \tag{9}$$

where $pO_{2,eq}K_{\mathrm{H}}$ is the equilibrium concentration of O_2 in water according to the temperature-dependent Henry's Constant.

2.6. Hypothesis Testing

We assessed normality in the data using quantile-quantile plots and Shapiro-Wilk Tests and heteroscedasticity in the data using Bartlett Tests for Homogeneity of Variance. CH_4, CO_2, and N_2O partial pressures and fluxes followed nonnormal distributions with unequal variances across sites and months. We compared means of partial pressures and fluxes across sites and months using nonparametric pairwise Wilcoxon signed rank t tests. We used a Bonferroni correction to an initial critical α value of 0.05 in order to compensate for loss in statistical power over subsequent comparisons (Zar, 2010). The corrected α for by-site and by-month comparisons was 0.025.

Our methods resulted in large sample sizes for each site (n ~ 36) and month (n ~ 72). To assess whether differences between means were independent of sample size and ecologically as well as statistically significant, we calculated effect sizes following Cohen (1988):

$$d = \frac{\mu_i - \mu_j}{\sqrt{\frac{\sigma_i^2 + \sigma_j^2}{2}}}, \tag{10}$$

where d is a descriptive measure corresponding to a small (0.0–0.4), medium (0.5–0.7), or large (0.8–2.0) effect size, μ is the mean of the sample, and σ is the standard deviation of the sample. Absolute Cohen's d values for effect size are reported with each α value.

2.7. Linear Mixed Effects Modeling

We investigated the diel ecosystem drivers of partial pressures and fluxes using linear mixed effects models (Table 1). Linear mixed effects models allowed these heteroscedastic data to vary independently across the

Table 1
Candidate Models and Number of Model Parameters (Including σ_ε) Used in Corrected Akaike Information Criterion Analyses, Grouped by Hypothesized Drivers of y_i

Model number	Model name	Model	Number of model parameters
1	Null	$y_i = (1\|g_i) \ldots + \varepsilon_y$	4
2	Partial in situ production	$y_i =$ hours since sunrise $+ (1\|g_i) + (0 + x_i\|g_i) \ldots + \varepsilon_y$	7
3	Full in situ production	$y_i =$ hours since sunrise + water temperature + dissolved O_2 + chlorophyll a $+ (1\|g_i) + (0 + x_i\|g_i) \ldots + \varepsilon_y$	16
4	Partial in situ respiration	$y_i =$ hours since sunset $(1\|g_i) + (0 + x_i\|g_i) \ldots + \varepsilon_y$	7
5	Full in situ respiration	$y_i =$ hours since sunset + water temperature + AOU + pH $+ (1\|g_i) + (0 + x_i\|g_i) \ldots + \varepsilon_y$	16

Note. Here, y_i is the partial pressure of CH_4, CO_2, or N_2O, diffusive flux of CH_4, CO_2, or N_2O, or CH_4 ebullition. The intercept and slope of each fixed effect, x_i, relative to each random effect, g_i, were allowed to vary independently as additional model parameters. Because inundation was measured during only one month, January, this random effect was omitted from the models describing drivers of diel partial pressures and fluxes on the submerged floodplain.

random effects of site and month. The slope of each fixed effect relative to each random effect was also allowed to vary independently following Bates et al. (2015):

$$y_i = \beta_{0,i} + \beta_i x_i \ldots + (1|g_i) + (0 + x_i|\, g_i) \ldots + \varepsilon_y, \tag{11}$$

where y_i is the partial pressure or flux; $\beta_{0,i}$ is the intercept of y_i; β_i is the coefficient for each effect, x_i; g_i is a random effect, such as site or month; and ε_y is the error associated with y_i. Small sample size-corrected Akaike Information Criterion (AIC_C) was used for model selection following Burnham and Anderson (2004). The likelihood of each model in describing partial pressures and diffusive fluxes relative to the other models was expressed in terms of ΔAIC_c and ΔAIC_c weight, w_i, following Burnham and Anderson (2004):

$$\Delta AIC_c = AIC_{c,i} - AIC_{c,\min}, \tag{12}$$

$$w_i = \frac{e^{-0.5\Delta AIC_{c,i}}}{\sum e^{-0.5\Delta AIC_{c,i}}}, \tag{13}$$

where $AIC_{c,\min}$ is the lowest AIC_c value in a group of candidate models. Candidate models for CH_4, CO_2, and N_2O partial pressures, CH_4, CO_2, and N_2O fluxes, and CH_4 ebullition, y_i, were designed according to hypothesized drivers. Model 1 was a null model, which included sampling site and month, only, as random effects with different intercepts.

Models 2 and 3 were nested in situ primary production models, which included hours since sunrise, water temperature, dissolved O_2, and chlorophyll a as fixed effects. Net primary production is typically greatest during the day (Odum, 1956), when photosynthesis produces dissolved O_2 and the photosynthetic pigment, chlorophyll a. Photosynthesis is also a temperature-dependent process (Farquhar et al., 1980).

Models 4 and 5 were nested in situ respiration models, which included hours since sunset, water temperature, AOU, and pH as fixed effects. Net respiration is typically greatest at night (Odum, 1956), when dissolved O_2 is consumed and CO_2 is produced in the absence of photosynthesis. Like photosynthesis, respiration is highly temperature dependent (Yvon-Durocher et al., 2012).

We assessed multicollinearity of fixed effects using Variance Inflation Factors (VIF) and bivariate Pearson Correlation Tests. VIF indicates the magnitude of variance among model coefficients, β_i, when a fixed effect, x_i, is included in a model. Where VIF > 5, the multicollinear fixed effect was tested against all other fixed effects in the model. Where a Pearson coefficient > 0.7 (r), the less ecologically relevant fixed effect for the hypothesized driver was omitted. For example, chlorophyll a and pH were found to be highly correlated in the full in situ primary production model ($r = 0.70$, $df = 201$, $p < 0.001$), so pH was omitted from this model.

3. Results

3.1. Magnitudes of Partial Pressures and Fluxes

3.1.1. Floodplain Ponds During Drawdown

Floodplain ponds were typically oversaturated with greenhouse gases relative to partial pressures sampled in ambient air, leading to diffusive emissions of CH_4, CO_2, and N_2O to the atmosphere (Table 2). There were

Table 2
Mean Diffusive Fluxes ($mg \cdot m^{-2} \cdot hr^{-1}$) ± SE and Partial Pressures (μatm) ± SE for CH_4, CO_2, and N_2O

Study Month, Site	n	CH_4 flux ($mg \cdot m^{-2} \cdot hr^{-1}$)	n	Ebullition ($mg \cdot m^{-2} \cdot hr^{-1}$)	n	pCH_4 (μatm)	n	CO_2 flux ($mg \cdot m^{-2} \cdot hr^{-1}$)	n	pCO_2 (μatm)	n	N_2O flux ($mg \cdot m^{-2} \cdot hr^{-1}$)	n	pN_2O (μatm)
June	67	2.2 ± 0.4	13	15 ± 4	12	50 ± 10	62	120 ± 20	12	160 ± 20	62	0.021 ± 0.009	12	0.37 ± 0.02
Natural	34	3.5 ± 0.7	9	18 ± 5	6	37 ± 9	30	80 ± 30	6	140 ± 20	32	0.030 ± 0.009	6	0.41 ± 0.01
Aquaculture	33	0.8 ± 0.3	4	9 ± 6	6	60 ± 20	32	170 ± 30	6	180 ± 40	30	0.01 ± 0.02	6	0.32 ± 0.02
August during rain	65	10 ± 1	6	19 ± 5	12	130 ± 20	65	15 ± 10	12	320 ± 70	65	0.03 ± 0.01	12	0.31 ± 0.02
Natural	32	12 ± 2	6	19 ± 5	6	114 ± 3	32	5 ± 18	6	250 ± 50	32	0.03 ± 0.01	6	0.35 ± 0.02
Aquaculture	33	8 ± 1	0		6	160 ± 30	33	30 ± 10	6	400 ± 100	33	0.03 ± 0.01	6	0.27 ± 0.01
August after rain	71	2.8 ± 0.6	12	6 ± 2	12	18 ± 2	71	14 ± 9	12	150 ± 20	71	0.009 ± 0.007	12	0.37 ± 0.02
Natural	35	5 ± 1	5	7 ± 2	6	18 ± 2	35	−10 ± 10	6	170 ± 30	35	−0.007 ± 0.006	6	0.37 ± 0.04
Aquaculture	36	1.0 ± 0.2	7	5 ± 2	6	18 ± 3	36	40 ± 20	6	130 ± 10	36	0.02 ± 0.01	6	0.36 ± 0.02
January	72	0.13 ± 0.05	14	0.09 ± 0.05	72	20 ± 10	72	28 ± 5	72	114 ± 8	72	0.004 ± 0.019	72	1.30 ± 0.03
Natural	36	−0.02 ± 0.03	1	0.1	36	5.4 ± 0.2	36	30 ± 5	36	110 ± 10	36	0.02 ± 0.01	36	1.29 ± 0.05
Aquaculture	36	0.30 ± 0.08	13	0.09 ± 0.06	36	30 ± 20	36	26 ± 8	36	120 ± 10	36	−0.01 ± 0.04	36	1.30 ± 0.05

Note. Mean ebullition ($mg \cdot m^{-2} \cdot hr^{-1}$) ± SE is also included. SE = standard error.

significant differences in pN_2O and diffusive CH_4 fluxes between natural and newly created aquaculture ponds on the Three Gorges Floodplain (Table 3). pN_2O was significantly greater in the natural pond in June ($p < 0.015$, $d = 1.9$) and August During Rain ($p < 0.009$, $d = 1.9$). During periods of no rain, diffusive CH_4 fluxes were also significantly greater in the natural pond than in the aquaculture pond ($p < 0.001$, $d = 0.8$ for June; $p = 0.001$, $d = 0.7$ for August After Rain). Effect sizes for these significant differences ranged from medium ($d = 0.5$–0.7) to high ($d \geq 0.8$), indicating both ecological and statistical significance (Cohen, 1988).

Precipitation had a significant effect on the partial pressures, diffusive fluxes, and ebullition of CH_4 in floodplain ponds. We observed significantly greater pCH_4 ($p < 0.001$, $d = 2.0$) and diffusive CH_4 fluxes ($p < 0.001$, $d = 0.9$) during rain in August than 3 days later, when the same sites were sampled again under conditions of no rain. Mean ebullition was also greater during rain in August (19 ± 5 $mg \cdot m^{-2} \cdot hr^{-1}$, $n = 6$) than after (6 ± 2 $mg \cdot m^{-2} \cdot hr^{-1}$, $n = 12$). Partial pressures and diffusive fluxes of CO_2 and N_2O were comparatively unaffected by this rain event.

Monthly and seasonal differences in greenhouse gas emissions measured in floodplain ponds and on the submerged floodplain following inundation by the Three Gorges Reservoir are shown as CO_2-equivalents in Figure 2. CO_2-equivalents were calculated over a 100-year time scale using CO_2 as a reference gas for global warming potential, where CH_4 has a global warming potential 25 times that of CO_2 and nitrous oxide has a global warming potential 298 times that of CO_2 (IPCC, 2001; Myhre et al., 2013). CH_4 diffusion and ebullition increased as a fraction of total CO_2-equivalents emitted by floodplain ponds from June to August, spiking to 98–99% during a rain event. CO_2 diffusion showed the opposite trend, and N_2O diffusion changed little throughout reservoir drawdown.

3.1.2. Submerged Floodplain During Inundation

Areal diffusive CH_4 fluxes were significantly lower on the submerged floodplain following inundation by the Three Gorges Reservoir ($p < 0.001$, $d = 0.7$; Figure 2). CH_4 ebullition also decreased significantly from reservoir drawdown to inundation ($p < 0.001$, $d = 1.4$). Little CH_4 was emitted through either diffusion or ebullition during inundation, when CO_2 and N_2O contributed 57–58% of total CO_2-equivalents emitted to the atmosphere.

3.2. Diel Patterns of Partial Pressures and Diffusive Fluxes

Oversaturation of CO_2 relative to the atmosphere corresponded with undersaturation of O_2 on the floodplain during both reservoir drawdown and inundation, consistent with net heterotrophy (Figure 3). The equimolar consumption of O_2 and production of CO_2 during aerobic respiration can be expressed as a slope of −1 when excess O_2 is regressed with excess CO_2. In both the natural and aquaculture ponds, these slopes were approximately −1, indicating in situ respiration as a key driver of pCO_2 ($r = -0.13$, $df = 15$, $p = 0.63$ for the natural pond and $r = -0.60$, $df = 15$, $p = 0.010$ for the aquaculture pond). This slope deviated from −1 on the

Table 3
Statistical Comparisons Between Natural and Aquaculture Ponds by Month

Study Month, Site	CH_4 Flux ($mg{\cdot}m^{-2}{\cdot}hr^{-1}$)	Ebullition ($mg{\cdot}m^{-2}{\cdot}hr^{-1}$)	pCH_4 (μatm)	CO_2 Flux ($mg{\cdot}m^{-2}{\cdot}hr^{-1}$)	pCO_2 (μatm)	N_2O Flux ($mg{\cdot}m^{-2}{\cdot}h^{-1}$)	pN_2O (μatm)
June	$p < 0.001$ $d = 0.8$***	NC	$p = 0.818$ $d = 0.4$	$p = 0.048$ $d = 0.5$	$p = 0.818$ $d = 0.4$	$p = 0.251$ $d = 0.6$	$p = 0.015$ $d = 1.9$***
August during rain	$p = 0.778$ $d = 0.3$	NC	$p = 0.065$ $d = 0.7$	$p = 0.151$ $d = 0.2$	$p = 0.485$ $d = 0.6$	$p = 0.092$ $d = 0.0$	$p = 0.009$ $d = 1.9$***
August after rain	$p = 0.001$ $d = 0.7$***	$p = 0.149$ $d = 0.4$	$p = 0.240$ $d = 0.1$	$p = 0.03$ $d = 0.6$	$p = 0.484$ $d = 0.6$	$p = 0.050$ $d = 0.6$	$p = 0.589$ $d = 0.2$
January	$p < 0.001$ $d = 0.8$***	NC	$p < 0.001$ $d = 0.3$*	$p = 0.838$ $d = 0.1$	$p = 0.775$ $d = 0.1$	$p = 0.574$ $d = 0.1$	$p = 0.376$ $d = 0.1$

Note. Means that are significantly different according to the Bonferroni-corrected α value are starred. Absolute Cohen's d values for effect size are also reported. Effect sizes typically ranged from medium (d = 0.5–0.7) to high (d > 0.8), indicating both ecological and statistical significance. Dissimilar samples sizes were not compared statistically (NC). Gray entries graphically show that results of hypothesis testing were not significant.
*Statistically significant with low effect size. ***Statistically significant with large effect size.

submerged floodplain following inundation by the Three Gorges Reservoir (*Slope* = 0.4; r = 0.28, df = 68, p = 0.021), indicating that other ecosystem processes were affecting pCO_2 (Crawford et al., 2014). Diffusive fluxes of CH_4, CO_2, or N_2O varied throughout the 24-hr sampling periods, along with dissolved O_2 and other fixed effects we associate with in situ primary production and in situ respiration (Figures 4 and S2). Five linear mixed effects models were used to determine whether in situ primary production and in situ respiration were more likely than a null model to drive observed patterns in greenhouse gas partial pressures and fluxes over diel time scales (Table 1).

3.3. Drivers of Partial Pressures and Fluxes

3.3.1. Floodplain Ponds During Drawdown

Diel partial pressures of CH_4, CO_2, and N_2O in water showed weak relationships with respective diel diffusive fluxes of CH_4 (r = 0.52, df = 84, p < 0.001), CO_2 (r = 0.11, df = 84, p = 0.310), and N_2O (r = −0.03, df = 84, p = 0.810). Because diel partial pressures of greenhouse gases in water were weakly related to diffusive fluxes in this study, diel partial pressures were modeled separately from diffusive fluxes. Diel partial pressures were not added as fixed effects in the modeling fluxes of diffusive fluxes.

We found that diel partial pressures of CH_4 and CO_2 in floodplain ponds were strongly supported by our full in situ respiration model, which included hours since sunset, water temperature, AOU, and pH as fixed effects (Table 4). pN_2O in floodplain ponds was best supported by the null model. Diel CO_2 fluxes in floodplain ponds were also driven by in situ respiration. This model was over 99% more likely to describe diel diffusive fluxes of CO_2 in floodplain ponds than in situ production or null models (see Weight, Table 5). Model fits for diel diffusive fluxes of CH_4 were inconclusive; relative support of diel CH_4 fluxes was divided between the null model (47%) and the partial in situ production model (51%), which included hours since sunrise as a fixed effect. Diffusive fluxes of N_2O in floodplain ponds were best supported by the null model.

3.3.2. Submerged Floodplain During Inundation

The relative importance of in situ respiration to diel partial pressures was consistent following inundation of the floodplain by the Three Gorges Reservoir. During inundation, diel pCH_4 and pCO_2 were still most strongly supported by the full in situ respiration model. However, relative support of pCO_2 by this model decreased from 93% to 86% from reservoir drawdown to inundation, consistent with the apparent decoupling of pCO_2 from dissolved O_2 dynamics observed from drawdown to inundation (Figure 3). Diel pN_2O was also most strongly supported by in situ respiration (partial model).

Like diel pCO_2, diel diffusive CO_2 fluxes were strongly supported by the in situ respiration model on the submerged floodplain following inundation by the Three Gorges Reservoir. During inundation, diel diffusive CH_4 and N_2O fluxes were best supported by the null model. Diel CH_4 ebullition was also more likely to be supported by the null model during both reservoir drawdown and inundation.

4. Discussion

4.1. pCH_4, pCO_2, and CO_2 Fluxes Varied on a Diel Basis With In Situ Respiration During Drawdown

Like other lentic environments on floodplains in Southeast Asia (Holtgrieve et al., 2013), West Africa (Kone et al., 2009), and Australia (Hunt et al., 2012), ponds on the Three Gorges Floodplain were heterotrophic (Figure 3). The accumulation of CH_4 and CO_2 within floodplain ponds varied on a diel basis with in situ

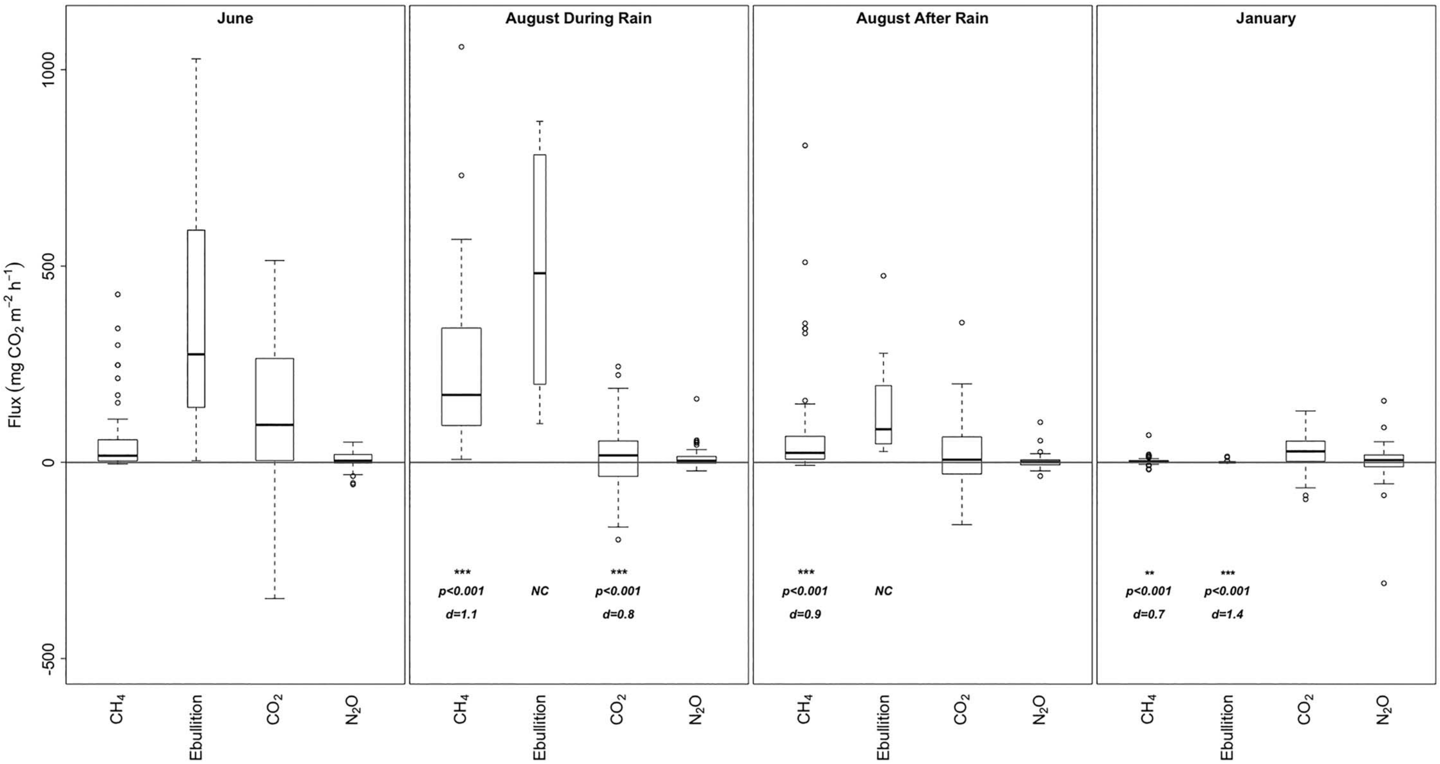

Figure 2. Fluxes of CH_4, CO_2, and N_2O expressed in mg CO_2-equivalents·m^{-2}·hr^{-1} in floodplain ponds during June and August and on the submerged floodplain following inundation by the Three Gorges Reservoir during January. The gray line at $y = 0$ delineates fluxes between these aquatic environments and the atmosphere. Width of boxes reflects relative sample size, which is smaller for ebullition (ranging from $n = 6$ to $n = 14$) than for diffusive fluxes (ranging from $n = 62$ to $n = 72$). Statistical and ecological significance across subsequent months is indicated by α values and absolute Cohen's d values for effect size. *Statistically significant with low effect size. **Statistically significant with medium effect size. ***Statistically significant with large effect size.

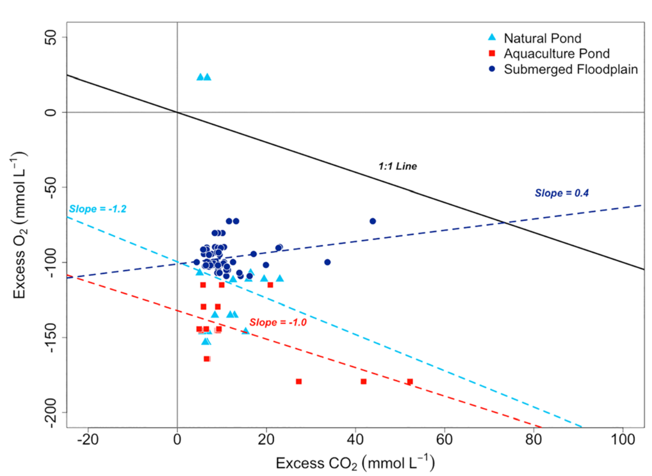

Figure 3. Saturation of O_2 and CO_2 in water relative to atmospheric equilibrium, at the gray lines or 0.0 mmol/L^1. The 1:1 line represents the equimolar consumption of O_2 and production of CO_2 during aerobic respiration. Slopes are the changes in excess dissolved O_2 relative to excess dissolved CO_2.

respiration according to linear mixed effects modeling, which included hours since sunset, water temperature, AOU, and pH as fixed effects. This model was over 92% more likely to explain observed diel variations in pCH$_4$, pCO$_2$, and diffusive CO_2 fluxes than the null model. Our approach and results are consistent with findings of Tobias et al. (2007), Hotchkiss and Hall (2014), and Schindler et al. (2017), who show that respiration rates can vary widely throughout the day. Thus, it may be necessary to measure pCH$_4$, pCO$_2$, and diffusive CO_2 fluxes on a diel basis in studies of not only stream and lake metabolism but also reservoir carbon cycling.

Respiration in the surrounding terrestrial landscape may have also contributed to significant increases in pCH$_4$ and diffusive CH_4 fluxes during precipitation and transfers of respiratory by-products from floodplain soils to ponds. During a rain event in August, diffusive CH_4 and ebullition fluxes spiked to 98–99% CO_2-equivalents emitted to the atmosphere from floodplain ponds. Ponds are intimately connected to the surrounding terrestrial landscape owing to comparatively high surface area-to-volume ratios (Holgerson, 2015). Terrestrial-aquatic transfers can enrich surface waters with by-products of soil respiration, increasing the partial pressures of CH_4 and CO_2 (Butman & Raymond, 2011; Kling et al., 1991; Raymond et al., 2016), or these flows can dilute surface water solute concentrations (Johnson et al., 2010). pCH$_4$ and diffusive CH_4 fluxes were significantly higher during rain than after rain, suggesting enrichment.

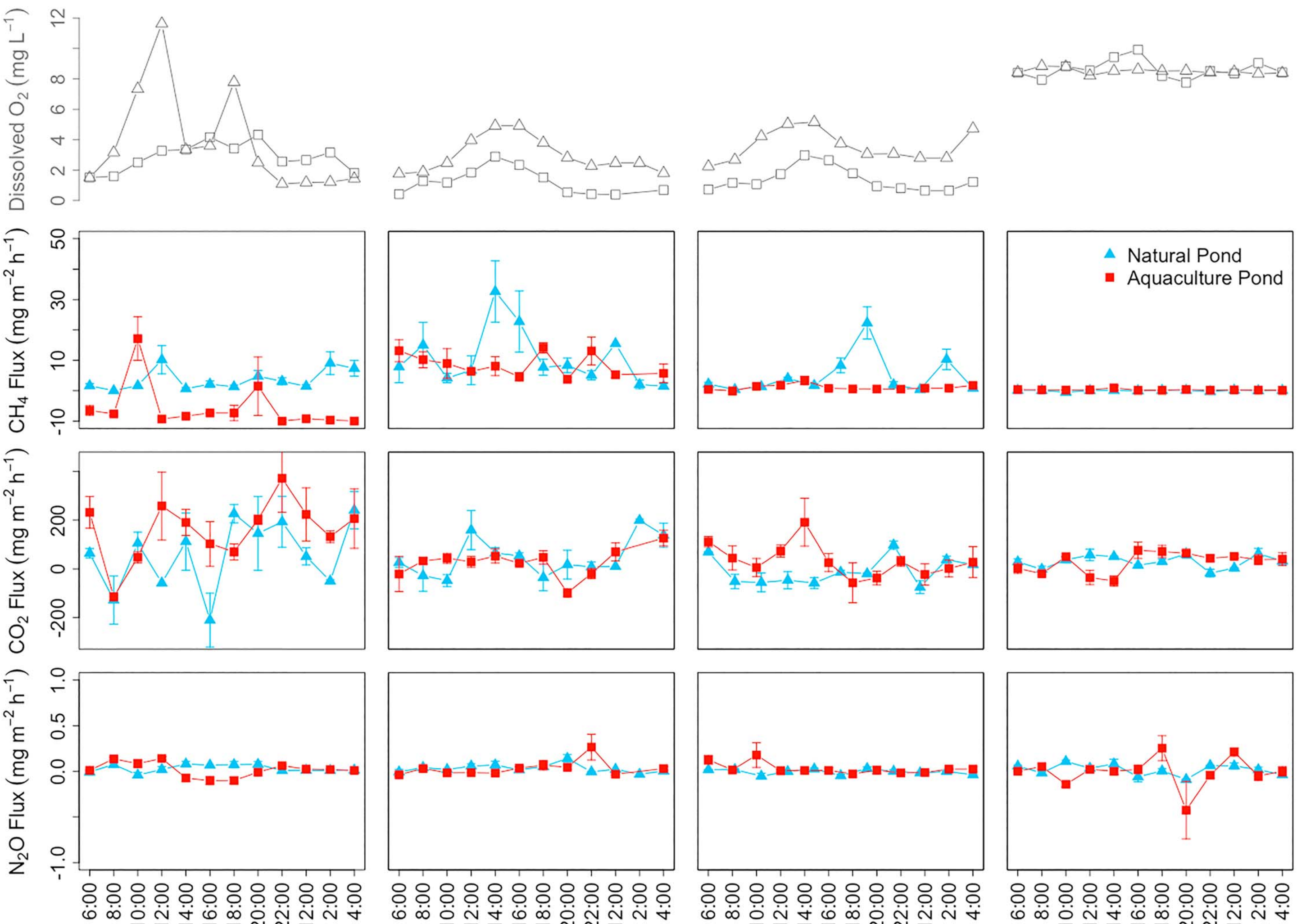

Figure 4. Diel variation in dissolved O_2 in natural and aquaculture ponds during each sampling event, compared with diel variation in diffusive CH_4, CO_2, and N_2O fluxes.

The onset of this rain event corresponded to a decrease in atmospheric pressure from 1,016 to 1,002 mbar, which may also explain observed significant increases in CH_4 ebullition (Ostrovsky et al., 2008).

4.2. Ebullition Was a Substantial Fraction of Total Drawdown Emissions

CH_4 ebullition comprised 60–68% of all CO_2-equivalents emitted from floodplain ponds to the atmosphere during reservoir drawdown (Figure 3). This is consistent with findings from the lake and reservoir literatures (Deemer et al., 2016; Del Sontro et al., 2010; Grinham et al., 2011; Maeck et al., 2014). Del Sontro et al. (2016) measured both the magnitude and drivers of ebullition in 10 northern temperate ponds. These ebullitive fluxes averaged 3.1 ± 0.7 mg $CH_4 \cdot m^{-2} \cdot hr^{-1}$, compared with the 15 ± 4, 19 ± 5, and 6 ± 2 mg $CH_4 \cdot m^{-2} \cdot hr^{-1}$ that we measured in June, August During Rain, and August After Rain, respectively (Table 2). The lower magnitude of ebullitive fluxes in ponds measured by Del Sontro et al. (2016) in northern temperate ponds may be due to the strong temperature dependence of respiration generally (Yvon-Durocher et al., 2012) and methanogenesis particularly in freshwater environments (Lofton et al., 2014; Schultz & Conrad, 1996; Segers, 1998; Yvon-Durocher et al., 2014). Temperatures ranged from 25 to 39 °C in our subtropical floodplain ponds and from 28 to 35 °C in their sediments, where ebullition originates. Del Sontro et al. (2016) found that sediment temperatures in their ponds rarely exceeded 25 °C and that ebullition was related to both sediment temperature and trophic status. Diel CH_4 ebullition in our study was not supported by our in situ production and in situ respiration models, suggesting other biotic and abiotic drivers during reservoir drawdown and inundation, such as atmospheric pressure.

Table 4
AIC_c Results for Five Candidate Models Predicting the Partial Pressures of CH_4, CO_2, and N_2O in Floodplain Ponds and the Submerged Floodplain

	Floodplain ponds			Submerged floodplain		
Model name	AIC_c	ΔAIC_c	Weight	AIC_c	ΔAIC_c	Weight
pCH$_4$	(df = 35)			(df = 71)		
Null model	368.58	26.95	0.000	841.55	34.62	0.000
Partial in situ production	364.39	22.76	0.000	837.30	30.37	0.000
Full in situ production	352.27	10.65	0.005	812.26	5.33	0.065
Partial in situ respiration	363.97	22.34	0.000	837.77	30.84	0.000
Full in situ respiration	341.61	0.00[a]	0.995[a]	806.93	0.00[a]	0.935[a]
pCO$_2$	(df = 35)			(df = 71)		
Null model	455.15	41.27	0.000	800.96	39.16	0.000
Partial in situ production	448.76	34.88	0.000	790.01	28.21	0.000
Full in situ production	418.96	5.07	0.073	765.36	3.56	0.144
Partial in situ respiration	444.96	31.07	0.000	793.09	31.29	0.000
Full in situ respiration	413.88	0.00[a]	0.927[a]	761.80	0.00[a]	0.856[a]
pN$_2$O	(df = 35)			(df = 71)		
Null model	−95.76	0.00[a]	0.743[a]	31.92	36.26	0.000
Partial in situ production	−92.15	3.61	0.122	18.63	22.96	0.000
Full in situ production	−65.72	30.04	0.000	27.93	32.26	0.000
Partial in situ respiration	−92.35	3.40	0.135	4.33	0.00[a]	0.948[a]
Full in situ respiration	−74.23	21.53	0.000	1.46	5.79	0.052

[a]Models with relative support (over two ΔAIC_c units).
AIC_c = corrected Akaike Information Criterion.

4.3. pCH$_4$ and CH$_4$ Fluxes Varied Seasonally, From Reservoir Drawdown to Floodplain Inundation

Diel pCH$_4$, pCO$_2$, and diffusive CO$_2$ fluxes were also driven by in situ respiration on the submerged floodplain following inundation by the Three Gorges Reservoir. Inundation did change the driver of diel pN$_2$O from other ecosystem processes during reservoir drawdown (indicated by strong support of the null model) to in situ respiration. Battin et al. (2008) and McNicol and Silver (2014) have each documented respiration of floodplain vegetation following inundation. The only plant species that survive seasonal flooding of the

Table 5
AIC_c Results for Six Candidate Models Predicting the Diffusive Fluxes of CH_4, CO_2, and N_2O From Floodplain Ponds and the Submerged Floodplain

	Floodplain ponds			Submerged floodplain		
Model name	AIC_c	ΔAIC_c	Weight	AIC_c	ΔAIC_c	Weight
Diffusive CH$_4$ fluxes	(df = 202)			(df = 71)		
Null model	1,337.29	0.14	0.472	70.12	0.00[a]	0.995[a]
Partial in situ production	1,337.15	0.00	0.507	81.96	11.85	0.003
Full in situ production	1,356.43	19.28	0.000	97.60	27.49	0.000
Partial in situ respiration	1,343.54	6.39	0.021	81.90	11.79	0.002
Full in situ respiration	1,352.23	15.08	0.000	95.92	25.81	0.000
Diffusive CO$_2$ fluxes	(df = 197)			(df = 71)		
Null model	2,861.12	17.11	0.000	915.37	11.94	0.002
Partial in situ production	2,861.35	17.33	0.000	917.48	14.05	0.001
Full in situ production	2,853.87	9.86	0.007	909.50	6.08	0.045
Partial in situ respiration	2,856.87	12.86	0.002	916.06	12.63	0.002
Full in situ respiration	2,844.01	0.00[a]	0.991[a]	903.43	0.00[a]	0.950[a]
Diffusive N$_2$O fluxes	(df = 198)			(df = 71)		
Null model	−530.07	0.00[a]	0.999[a]	−67.56	0.00[a]	0.997[a]
Partial in situ production	−514.27	66.14	0.000	−54.63	12.93	0.002
Full in situ production	−463.93	66.14	0.000	−30.92	36.64	0.000
Partial in situ respiration	−514.81	15.26	0.001	−54.19	13.37	0.001
Full in situ respiration	−475.58	54.49	0.000	−31.71	35.84	0.000

[a]Models with relative support (over two ΔAIC_c units).
AIC_c = corrected Akaike Information Criterion.

Pengxi River Wetland Reserve are the grasses *Cynodon dactylon* and *Echinochloa crusgali* var. *zelayensis* and the legume *Aeschynomene indica* (Wang et al., 2009). Remaining terrestrial vegetation in the reserve dies following inundation, including the lotus (*Nelumbo nucifera*) cultivated in aquaculture ponds. Seasonal senescence of many aquatic and terrestrial plant species on the Three Gorges Floodplain likely provides ample substrates for in situ respiration following inundation.

Interestingly, the magnitudes of CH_4 emissions alone seemed affected by inundation. Diffusive CH_4 fluxes and CH_4 ebullition decreased significantly from 2.8 ± 0.5 and 6 ± 2 $mg \cdot m^{-2} \cdot hr^{-1}$, respectively, during reservoir drawdown to 0.13 ± 0.05 and 0.09 ± 0.05 $mg \cdot m^{-2}\ hr^{-1}$ during inundation. pCO_2, pN_2O, and the diffusive fluxes of CO_2 and N_2O per square meter were not significantly different from reservoir drawdown to inundation in January. This meant that diffusive CO_2 and N_2O fluxes were proportionately more important to total CO_2-equivalents emitted per unit area during inundation than during reservoir drawdown. The decrease in areal CH_4 emissions during inundation may be due to a combination of lower temperatures and higher O_2 saturation on the submerged floodplain following inundation by the Three Gorges Reservoir. During winter inundation, water temperatures in on the submerged floodplain ranged from 13 to 14 °C compared to 25 to 39 °C in floodplain ponds during summer reservoir drawdown. Fewer CH_4 bubbles may have been produced in colder submerged floodplain sediments. During inundation, inverted funnels in deeper, colder water (16–25 m) also captured much smaller magnitudes of ebullition than floating chambers in shallower water (<2 m; $p < 0.001$, $d = 1.4$), which is consistent with other studies (Del Sontro et al., 2016; Deshmukh et al., 2014). Furthermore, dissolved O_2 on the submerged floodplain was significantly greater than during drawdown in floodplain ponds ($p < 0.001$, $d = 2.0$; Figure 4), sometimes approaching 98% saturation. Dissolved CH_4 may have been oxidized within this more oxic water column (Guerin & Abril, 2007). Therefore, both inundation and the season in which it occurs likely contributed to our observed decreases in diffusive CH_4 fluxes and CH_4 ebullition.

No other studies in the Three Gorges Reservoir have measured ebullition, meaning that spatial coverage is limited to our study, 14 inverted funnels, a small area of the submerged floodplain, and one January sampling event over 2 days thus far. Wik et al. (2016) estimated that 11 inverted funnels and 39 days of sampling were required in northern temperate lakes encompassing 0.02–0.17 km^2 in order to accurately (±20%) measure ebullition captured by 17 funnels over 62 days. Lower spatial and temporal coverage most often results in underestimates of ebullition (Wik et al., 2016). This makes greater coverage and more accurate ebullition estimates for the Three Gorges Reservoir a priority for future studies.

4.4. Partial Pressures Were Weakly Related to Diffusive Fluxes

The modeled diffusive flux of any gas between water and the atmosphere is a function of its concentration gradient between water and the atmosphere and the gas transfer velocity. Yet, partial pressures of CH_4, CO_2, and N_2O in water were weakly related to our measured diffusive fluxes. This indicates the importance of the gas transfer velocity, which depends largely on turbulence at the interface between water and the atmosphere (Banerjee & MacIntyre, 2004; McGillis et al., 2004). Turbulence on the surface of ponds and reservoirs can result from convection or wind speed, which are positively correlated to diffusive flux (MacIntyre et al., 2010). Diffusive CH_4 fluxes measured by this study were slightly more related to the gas transfer velocity ($r = 0.60$, $df = 84$, $p = 0.016$) than to partial pressures of CH_4 ($r = 0.52$, $df = 84$, $p < 0.001$). This was not true for diffusive CO_2 and N_2O fluxes. It is generally assumed and in some cases empirically shown (Natchimuthu et al., 2017) that partial pressures are highly correlated to diffusive fluxes. Other studies by Schilder et al. (2013) in lakes and Crawford et al. (2015) in streams have shown weak relationships between partial pressures and diffusive fluxes and stronger relationships between diffusive fluxes and the gas transfer velocity. Our results and others suggest that synoptic observations of partial pressures do not always predict the magnitudes of diffusive fluxes. Further comparisons between partial pressures of CH_4, CO_2, and N_2O in water and the diffusive fluxes measured by floating chambers are needed, particularly when partial pressures are widely used to model diffusive fluxes when not directly measured by chambers.

4.5. Ponds on the Three Gorges Floodplain Were Sizeable CH_4 Emitters

We used the Institute for Scientific Information Web of Science to review other studies reporting diffusive CH_4, CO_2, and N_2O fluxes from aquatic and terrestrial environments on the Three Gorges Floodplain and in the Three Gorges Reservoir. During reservoir drawdown, these environments included ponds,

Table 6
Mean Diffusive CH_4, CO_2, and N_2O Fluxes, in mg CO_2-Equivalents ± Standard Error, Reported by Other Studies in Aquatic and Terrestrial Environments on the Three Gorges Floodplain, Yangtze River, and Its Tributaries During Reservoir Drawdown

Ecosystem type	Month	CH_4 flux (mg $CO_2 \cdot m^{-2} \cdot hr^{-1}$)	CO_2 flux (mg $CO_2 \cdot m^{-2} \cdot hr^{-1}$)	N_2O flux (mg $CO_2 \cdot m^{-2} \cdot hr^{-1}$)	Source
Three Gorges Floodplain					
Schoenoplectus triqueter wetland	July–September	373 ± 273		15 ± 18	Chen, Wu, et al., 2009; Chen, Yuan, et al., 2009
Juncus amuricus wetland	July–September	6 ± 16		6 ± 15	Chen, Wu, et al., 2009; Chen, Yuan, et al., 2009
Typha augustifolia wetland	July–September	16 ± 28		6 ± 6	Chen, Wu, et al., 2009; Chen, Yuan, et al., 2009
Paspalum distichum wetland	July–September	170 ± 125		9 ± 12	Chen, Wu, et al., 2009; Chen, Yuan, et al., 2009
Oryza sativa wetland	June	122 ± 58			Lu et al., 2011
Aquaculture pond	June	4 ± 1			Zhou et al., 2017
Aquaculture pond	June	20 ± 8	168 ± 29	3 ± 6	This study
Natural pond	June	35 ± 13		3 ± 12	Zhou et al., 2017
Natural pond	June	88 ± 18	78 ± 32	9 ± 3	This study
Aquaculture pond	August	113 ± 20	38 ± 14	3 ± 3	This study
Natural pond	August	175 ± 25	6 ± 15	6 ± 3	This study
Grasslands	July–September	7 ± 2			Chen, Wu, et al., 2009; Chen, Yuan, et al., 2009
Grasslands	June	−1 ± 1			Yang et al., 2012
Grasslands	June	18 ± 8		21 ± 9	Zhou et al., 2017
Forests	June	0.3 ± 0.9			Yang et al., 2012
Forests	June	13 ± 8			Zhou et al., 2017
Agricultural lands	June	−0.3 ± 0.8			Yang et al., 2012
Agricultural lands	June	150 ± 50			Zhou et al., 2017
	April	2 ± 2			Xiao et al., 2013
Yangtze River and tributaries					
Yangtze River	June	8 ± 23			Lu et al., 2012
Yangtze River	July	13 ± 13			Yang et al., 2013
Yangtze River	August	1.5 ± 0.5			Xiao et al., 2013
Tributary	April	8 ± 2			Xiao et al., 2013
Tributary	June		−47 ± 22		Zhao et al., 2013
Tributary	July	6 ± 2			Chen, Wu, et al., 2009
Tributary	July		−90 ± 18		Zhao et al., 2013
Tributary	August	2.3 ± 0.5			Xiao et al., 2013

wetlands, the Yangtze River, its tributaries, grasslands, forests, and agricultural lands. During inundation, these environments included the mainstem Three Gorges Reservoir and its submerged floodplain. Fluxes were converted to mg CO_2-equivalents$\cdot m^{-2} \cdot day^{-1}$ ± Standard Error of the mean for comparison across environments (Tables 6 and 7). The surface areas occupied by each environment during reservoir drawdown and inundation are presented in Table 8 (Chen, Yuan, et al., 2009; Zhang et al., 2018). Studies that did not specify sampling month or environment were omitted.

We found that most studies measure diffusive CH_4 fluxes, only. Ponds and wetlands have the highest diffusive CH_4 emissions per square meter on the Three Gorges Floodplain during reservoir drawdown (Table 6), meaning that recent expansion of ponds for aquaculture on the Three Gorges Floodplain is likely increasing diffusive CH_4 emissions (Li et al., 2013; Zhang et al., 2018; Zhou et al., 2017). Grasslands, forests, and agricultural lands measured by other studies on the Three Gorges Floodplain were also sources for diffusive CH_4 to the atmosphere. Globally, terrestrial soils are typically CH_4 sinks (Smith et al., 2000). However, CH_4 oxidation rates in terrestrial soils are diminished by porewater content and landscape disturbances like agriculture (Smith et al., 2000). Both high porewater content and landscape disturbances can be expected on a humid, monsoonal, and historically densely populated Three Gorges Floodplain now undergoing seasonal inundation. Published diffusive CH_4 fluxes for the Yangtze River and its tributaries during reservoir drawdown show that these environments are essentially CH_4 neutral.

Table 7
Mean Diffusive CH_4, CO_2, and N_2O Fluxes, in mg CO_2-Equivalents ± Standard Error, Reported in the Mainstem Three Gorges Reservoir and Its Submerged Floodplain During Inundation

Ecosystem type	Month	CH_4 flux (mg $CO_2 \cdot m^{-2} \cdot hr^{-1}$)	CO_2 flux (mg $CO_2 \cdot m^{-2} \cdot hr^{-1}$)	N_2O flux (mg $CO_2 \cdot m^{-2} \cdot hr^{-1}$)	Source
Three Gorges Reservoir					
Main stem reservoir	January	5 ± 3			Yang et al., 2013
Main stem reservoir	February	0.5 ± 0.3			Xiao et al., 2013
Main stem reservoir	October	1.0 ± 0.8			Xiao et al., 2013
	January-April	8 ± 10			Chen et al., 2011
Submerged floodplain					
Submerged wetlands					
Submerged aquaculture pond	January	8 ± 2	30 ± 9	−3 ± 9	This study
Submerged natural pond	January	−1 ± 1			Zhou et al., 2017
Submerged natural pond	January	0.5 ± 0.8	33 ± 5	6 ± 3	This study
Submerged grasslands	November	5 ± 8			Yang et al., 2012
Submerged grasslands	January	−1 ± 2			Zhou et al., 2017
Submerged forests	November	5 ± 5			Yang et al., 2012
Submerged agricultural lands	November	10 ± 10			Yang et al., 2012
Submerged agricultural lands	January	13 ± 8			Zhou et al., 2017
Submerged tributary	January–April		111 ± 11		Li et al., 2014
Submerged tributary	January–April	5 ± 10			Chen et al., 2011
Submerged tributary	March		−13 ± 4		Zhao et al., 2013
Submerged tributary	October	2.0 ± 0.5			Xiao et al., 2013

Aquatic and terrestrial floodplain environments during reservoir drawdown (comprising a total surface area of 1,053.3 km^2) tend to have higher diffusive CH_4 fluxes per square meter than the surface of both the mainstem Three Gorges Reservoir and submerged floodplain during inundation (1,106.2 km^2; Tables 6–8). Diffusive CH_4 fluxes range from −1 ± 1 mg CO_2-equivalents$\cdot m^{-2} \cdot day^{-1}$ in grasslands to 373 ± 273 mg CO_2-equivalents$\cdot m^{-2} \cdot day^{-1}$ in wetlands during drawdown. These fluxes range from −1 ± 1 mg CO_2-equivalents$\cdot m^{-2} \cdot day^{-1}$ in submerged grasslands to 13 ± 8 mg CO_2-equivalents$\cdot m^{-2} \cdot day^{-1}$ in submerged agricultural lands during inundation.

Table 8
Surface Areas of Aquatic and Terrestrial Environments in the Three Gorges region, in Square Kilometers

Environment	Surface Area (km^2)	Source
Reservoir drawdown		
Ponds	100.0	Unavailable
Wetlands		Chen, Wu, et al., 2009
Yangtze River and tributaries	784.8	Chen, Wu, et al., 2009; Zhang et al., 2018
Grasslands	15.1	Zhang et al., 2018
Forests	63.8	Zhang et al., 2018
Agricultural lands	89.6	Zhang et al., 2018
Building lands	52.9	Zhang et al., 2018
Inundation		
Main stem reservoir	784.8	Chen, Wu, et al., 2009; Zhang et al., 2018
Submerged floodplain	321.4	Chen, Wu, et al., 2009; Zhang et al., 2018

Note. Surface areas during reservoir drawdown (Three Gorges Floodplain, Yangtze River, and Tributaries) total 1,053.3 km^2, not including 52.9 km^2 of urban and suburban areas (Zhang et al., 2018). Surface areas during inundation (Three Gorges Reservoir and Submerged Floodplain) total 1,602.1 km^2.

Comparisons of diffusive CH_4 emissions from aquatic and terrestrial floodplain environments during reservoir drawdown and from the main stem reservoir and submerged floodplain during inundation come with two important caveats. The first is that data from the literature include few measurements of diffusive CO_2 fluxes and no estimates of terrestrial primary production in grasslands, forests, and agricultural lands during reservoir drawdown. Each of these ecosystems is likely to sequester considerable quantities of CO_2. Based on the negative diffusive CO_2 fluxes reported in the literature, tributaries are also net autotrophic. In a study by Zhao et al. (2013), for example, it was found that the Yangtze River and its tributaries have the potential to sequester up to 90 ± 18 mg $CO_2 \cdot m^{-2} \cdot hr^{-1}$ during reservoir drawdown. During late summer (August), we also found that natural floodplain ponds also have the potential to sequester comparatively small amounts (−10 ± 10 to 5 ± 18 mg$\cdot m^{-2} \cdot hr^{-1}$) of CO_2, perhaps due to primary production. Indeed, chlorophyll *a* was significantly higher in the natural pond than in the aquaculture pond ($p < 0.001$, $d = 2.0$). More diffusive CO_2 flux measurements are needed in both aquatic and terrestrial floodplain environments during reservoir drawdown and inundation to adequately assess the complete C balance of the region under its new and dynamic hydrologic regime.

Second, the fate of CH_4 stored in the large water volumes of the mainstem Three Gorges Reservoir and its submerged floodplain is unknown.

Though diffusive CH_4 emissions are comparatively low from the surface of the reservoir during inundation, total water volumes increase from 17.2 km^3 during drawdown to 39.9 km^3 during this period (Wang et al., 2014). CH_4 can be stored at higher concentrations in the anoxic layer of vertically stratified lakes and reservoirs and then released via diffusion during periods of overturn and mixing (Beaulieu et al., 2014; Michmerhuizen et al., 1996; Riera et al., 1999). We sampled dissolved CH_4 from the surfaces of the Three Gorges Reservoir, only. Using these mean concentrations, the water level-water volume relationship reported by Wang et al. (2014) for the Three Gorges region, and assuming that the water column is uniformly mixed, we can extrapolate that the Three Gorges Reservoir stores 8 $\pm$ 1 kg CH_4 during the winter, when pCH_4 and diffusive CH_4 emissions are comparatively low. By comparison, the Three Gorges Floodplain, Yangtze River, and its tributaries may store up to 3.6 $\pm$ 0.7 kg CH_4 during reservoir drawdown in August, when diffusive emissions are comparatively high, using CH_4 concentrations measured in floodplain ponds and a local tributary (Pengxi River). The fate of the larger quantities of dissolved CH_4 in the Three Gorges Reservoir during reservoir overturn and downstream export is unclear. Drops in hydrostatic pressure during the transition from peak inundation to reservoir drawdown may also result in bubble release from reservoir sediments and additional CH_4 emissions (Beaulieu et al., 2018; Harrison et al., 2017). Reservoir overturn, downstream export, and drops in hydrostatic pressure each constitute "hot moments" for CH_4 emissions, which are important to reservoir C balances though difficult to capture via synoptic field sampling (Deemer et al., 2016). Irrespective of ultimate atmospheric CH_4 contributions by the Three Gorges Reservoir, our study and other studies show that ponds and wetlands on the Three Gorges Floodplain during reservoir drawdown are also sizeable sources for diffusive CH_4 to the atmosphere.

5. Conclusions

Our study shows that it is critical to consider how drawdown and inundation tie C and N cycling in hydropower reservoirs to their floodplains. Greenhouse gas emissions resulting from this C and N cycling are temporally dynamic. This is due not just to the association of greenhouse gas production with diel ecosystem metabolism but also with the seasonal disturbance regime of inundation. The Three Gorges Dam is one case study in a global hydropower boom (Zarfl et al., 2015) that is altering the hydrologic regime, frequency and scale of inundation, and balance of autotrophic and heterotrophic processes within river basins. We show that the drawdown/inundation cycle on the Three Gorges Floodplain changes the magnitudes of greenhouse gas fluxes from one of the world's largest reservoirs to the atmosphere and that certain environments on reservoir floodplains during drawdown can be nontrivial sources for CH_4.

Acknowledgments
This work was partially supported by the National Science Foundation East Asia-Pacific Summer Research Grant 1310724, the National Science Foundation Graduate Research Fellowship Grant DGE1256260, the National Science Foundation Earth Science Research Grant 1740042, the 100 Talents of the Chinese Academy of Sciences, and the Chinese Science and Technology Exchange Council. Evan V. Arntzen provided critical support during field sampling. We also thank Matthew J. Bogard and four anonymous reviewers for helpful comments during the preparation of this manuscript. All data and data products presented in figures and analyses are available online (https://github.com/blm8/Three-Gorges-Floodplain.git).

References

Alin, S. R., de Fatima, M., Rasera, F. L., Salimon, C. I., Richey, J. E., Holtgrieve, G. W., et al. (2011). Physical controls on carbon dioxide transfer velocity and flux in low-gradient river systems and implications for regional carbon budgets. *Journal of Geophysical Research*, *116*, G01009. https://doi.org/10.1029/2010JG001398

Aufdenkampe, A. K., Mayorga, E., Raymond, P. A., Melack, J. M., Doney, S. C., Alin, S. R., et al. (2011). Riverine coupling of biogeochemical cycles between land, oceans, and atmosphere. *Frontiers In Ecology and the Environment*, *9*(1), 53–60. https://doi.org/10.1890/100014

Bains, S. B., & Pace, M. L. (1991). The production of dissolved organic matter by phytoplankton and its importance to bacteria: Patterns across marine and freshwater systems. *Limnology and Oceanography*, *36*(6), 1078–1090. https://doi.org/10.4319/lo.1991.36.6.1078

Banerjee, S., & MacIntyre, S. (2004). The air-water interface—Turbulence and scalar exchange. In J. Grue, et al. (Eds.), *Advances in coastal and ocean engineering*, (9th ed.pp. 181–237). Hackensack, N.J: World Scientific Publishing.

Barros, N., Cole, J. J., Tranvik, L. J., Prairie, Y. T., Bastviken, D., Huszar, V. L. M., et al. (2011). Carbon emission from hydroelectric reservoirs linked to reservoir age and latitude. *Nature Geoscience*, *4*(9), 593–596. https://doi.org/10.1038/NGEO1211

Bastviken, D., Cole, J., Pace, M., & Tranvik, L. (2004). Methane emissions from lakes—Dependence of lake characteristics, two regional assessments, and a global estimate. *Global Biogeochemical Cycles*, *18*, GB4009. https://doi.org/10.1029/2004GB002238

Bastviken, D., Santoro, A. L., Marotta, H., Pinho, L. Q., Calheiros, D. F., Crill, P., & Enrich-Prast, A. (2010). Methane emissions from Pantanal, South America, during the low water season: Toward more comprehensive sampling. *Environmental Science and Technology*, *44*(14), 5450–5455. https://doi.org/10.1021/es1005048

Bates, D., Maechler, M., Bolker, B., & Walker, S. (2015). Fitting linear mixed effects models using lme4. *Journal of Statistical Software*, *67*(7), 1–36. https://doi.org/10.18637/jss.v067.i07

Battin, T. J., Kaplan, L. A., Findlay, S., Hopkinson, C. S., Marti, E., Packman, A. I., et al. (2008). Biophysical controls on organic carbon fluxes in fluvial networks. *Nature Geoscience*, *1*(2), 95–100. https://doi.org/10.1038/ngeo101

Beaulieu, J. J., Balz, D. A., Birchfield, M. K., Harrison, J. A., Nietch, C. T., Platz, M. C., et al. (2018). Effects of an experimental water-level drawdown on methane emissions from a eutrophic reservoir. *Ecosystems*, *21*(4), 657–674. https://doi.org/10.1007/s10021-017-0176-2

Beaulieu, J. J., Smolenski, R. L., Nietch, C. T., Townsend-Small, A., Elovitz, M. S., & Schubauer-Berigan, J. P. (2014). Denitrification alternates between a source and sink of nitrous oxide in the hypolimnion of a thermally stratified reservoir. *Limnology and Oceanography*, *59*(2), 495–506. https://doi.org/10.4319/lo.2014.59.2.0495

Burnham, K. P., & Anderson, D. R. (2004). Multimodel inference—Understanding AIC and BIC in model selection. *Sociological Methods and Research*, *33*(2), 261–304. https://doi.org/10.1177/0049124104268644

Burns, A., & Ryder, D. S. (2001). Response of bacterial extracellular enzymes to inundation of floodplain sediments. *Freshwater Biology*, *46*, 1299–1307. https://doi.org/10.1046/j.1365-2427.2001.00750.x

Butman, D., & Raymond, P. A. (2011). Significant efflux of carbon dioxide from streams and rivers in the United States. *Nature Geoscience*, *4*(12), 839–842. https://doi.org/10.1038/ngeo1294

Chen, H., Wu, Y., Yuan, X., Gao, Y., Wu, N., & Zhu, D. (2009). Methane emissions from newly created marshes in the drawdown area of the Three Gorges Reservoir. *Journal of Geophysical Research*, *114*(D18), D18301. https://doi.org/10.1029/2009JD012410

Chen, H., Yuan, X., Chen, Z., Wu, Y., Liu, X., Zhu, D., et al. (2011). *Methane emissions from the surface of the Three Gorges Reservoir*, *116*, D21306. https://doi.org/10.1029/2011Jd016244

Chen, H., Yuan, X., Gao, Y., Wu, N., Zhu, D., & Wang, J. (2009). Nitrous oxide emissions from newly created littoral marshes in the drawdown area of the Three Gorges Reservoir, China. *Water, Air, and Soil Pollution*, *211*(1-4), 25–33. https://doi.org/10.1007/s11270-009-0277-4

Cohen, J. (1988). *Statistical power analysis for the behavioral sciences*, (2nd ed.). Hillsdale, New Jersey: Lawrence Earlbaum Associates.

Cole, J. J., Likens, G. E., & Strayer, D. L. (1982). Photosynthetically produced dissolved organic carbon: An important source for planktonic bacteria. *Limnology and Oceanography*, *27*(6), 1080–1090. https://doi.org/10.4319/lo.1982.27.6.1080

Crawford, J. T., Dornblaser, M. M., Stanley, E. H., Clow, D. W., & Striegl, R. G. (2015). Source limitation of carbon gas emissions in high-elevation mountain streams and lakes. *Journal of Geophysical Research: Biogeosciences*, *120*, 952–964. https://doi.org/10.1002/2014JG002861

Crawford, J. T., Lottig, N. R., Stanley, E. H., Walker, J. F., Hanson, P. C., Finlay, J. C., & Striegl, R. G. (2014). CO_2 and CH_4 emissions from streams in a lake-rich landscape—Patterns, controls, and regional significance. *Global Biogeochemical Cycles*, *28*, 197–210. https://doi.org/10.1002/2013GB004661

Deemer, B., Harrison, J. A., Li, S., Beaulieu, J. J., Del Sontro, T., Barros, N., et al. (2016). Greenhouse gas emissions from reservoir water surfaces: A new global synthesis. *BioScience*, *66*(11), 949–964. https://doi.org/10.1093/biosci/biw117

Deemer, B. R., Harrison, J. A., & Whitling, E. W. (2011). Microbial dinitrogen and nitrous oxide production in a small eutrophic reservoir: An in situ approach to quantifying hypolimnetic process rates. *Limnology and Oceanography*, *56*(4), 1189–1199. https://doi.org/10.4319/lo.2011.56.4.1189

Del Sontro, T., Boutet, L., Pierre, A. S., del Giorgio, P. A., & Prairie, Y. T. (2016). Methane ebullition and diffusion from northern ponds and lakes regulated by the interaction between temperature and system productivity. *Limnology and Oceanography*, *61*(S1), S62–S77. https://doi.org/10.1002/lno.10335

Del Sontro, T., Kunz, M. J., Kempter, T., Wuest, A., Wehrli, B., & Senn, D. B. (2011). Spatial heterogeneity of methane ebullition in a large tropical reservoir. *Environmental Science and Technology*, *45*, 9866–9873. https://doi.org/10.1021/es205545

Del Sontro, T., McGinnia, D. F., Sobek, S., Ostrovsky, I., & Wehrli, B. (2010). Extreme methane emissions from a Swiss hydropower reservoir: Contribution from bubbling sediments. *Environmental Science and Technology*, *44*, 2419–2425. https://doi.org/10.1021/es9031369

Deshmukh, C., Serca, D., Delon, C., Tardiff, R., Demarty, M., Jarnot, C., et al. (2014). Physical controls on CH_4 emissions from a newly flooded subtropical freshwater hydroelectric reservoir—Nam Theun 2. *Biogeosciences*, *11*(15), 4251–4269. https://doi.org/10.5194/bg-11-4251-2014

Farquhar, G. D., von Caemmerer, S., & Berry, J. A. (1980). A biochemical model of photosynthetic CO_2 assimilation in leaves of C3 plants. *Planta*, *149*(1), 78–90. https://doi.org/10.1007/BF00386231

Fendinger, N. J., Adams, D. D., & Glotfelty, D. E. (1992). The role of gas ebullition in the transport of organic contaminants from sediments. *Science of the Total Environment*, *112*(2-3), 189–201. https://doi.org/10.1016/0048-9697(92)90187-W

Frankignoulle, M. (1988). Field measurements of air-sea CO_2 exchange. *Limnology and Oceanography*, *33*(3), 313–322. https://doi.org/10.4319/lo.1988.33.3.0313

Galy-Lacaux, C., Delmas, R., & Jambert, C. (1997). Gaseous emissions and oxygen consumption in hydroelectric dams: A case study in French Guyana. *Global Biogeochemical Cycles*, *11*(4), 471–483. https://doi.org/10.1029/97GB01625

Grinham, A., Albert, S., Deernis, N., Dunbabin, M., Bastviken, D., Sherman, B., et al. (2018). The importance of small artificial water bodies as sources of methane emissions in Queensland, Australia. *Hydrology and Earth Systems Sciences*, *22*, 5281–5298. https://doi.org/10.5194/hess-22-5281-2018

Grinham, A., Dunbabin, M., Gale, D., & Udy, J. (2011). Quantification of ebullitive and diffusive methane release to atmosphere from a water storage. *Atmospheric Environment*, *45*(39), 7166–7173. https://doi.org/10.1016/j.atmosenv.2011.09.011

Guerin, F., & Abril, G. (2007). Significance of pelagic aerobic methane oxidation in the methane and carbon budget of a tropical reservoir. *Journal of Geophysical Research—Biogeosciences*, *112*, G03006. https://doi.org/10.1029/2006JG000393

Guerin, F., Abril, G., Tremblay, A., & Delmas, R. (2008). Nitrous oxide emissions from tropical hydropower reservoirs. *Geophysical Research Letters*, *35*, L06404. https://doi.org/10.1029/2007GL033057

Harrison, J. A., Deemer, B. R., Birchfield, M. K., & O'Malley, M. T. (2017). Reservoir water-level drawdowns accelerate and amplify methane emission. *Environmental Science and Technology*, *51*(3), 1267–1277. https://doi.org/10.1021/acs.est.6b03185

Hayes, N. M., Deemer, B. R., Corman, J. R., Roxanna Razavi, N., & Strock, K. E. (2017). Key differences between lakes and reservoirs modify climate signals—A case for a new conceptual model. *Limnology and Oceanography—Letters*, *2*(2), 47–62. https://doi.org/10.1002/lol2.10036

Hoellein, T. J., Bruesewitz, D. A., & Richardson, D. C. (2013). Revisiting Odum (1956): A synthesis of aquatic ecosystem metabolism. *Limnology and Oceanography*, *58*(6), 2089–2100. https://doi.org/10.4319/lo.2013.58.6.2089

Holgerson, M. A. (2015). Drivers of carbon dioxide and methane supersaturation in small, temporary ponds. *Biogeochemistry*, *124*(1-3), 305–318. https://doi.org/10.1007/s10533-015-0099-y

Holgerson, M. A., & Raymond, P. A. (2016). Large contribution to inland water CO_2 and CH_4 emissions from very small ponds (2016). *Nature Geoscience*, *9*(3), 222–226. https://doi.org/10.1038/ngeo2654

Holtgrieve, G. W., Arias, M. E., Irvine, K. N., Lamberts, D., Ward, E. J., Kummua, M., et al. (2013). Patterns of ecosystem metabolism in the Tonle Sap Lake, Cambodia with links to capture fisheries. *PLOS ONE*, *8*(8), e71395. https://doi.org/10.1371/journal.pone.0071395.g001

Hotchkiss, E. R., & Hall, R. O. Jr. (2014). High rates of daytime respiration in three streams: Use of $\delta^{18}O_{O2}$ and O_2 to model diel ecosystem metabolism. *Limnology and Oceanography*, *59*(3), 798–810. https://doi.org/10.4319/lo.2014.59.3.0798

Hunt, R. J., Jardine, T. D., Hamilton, S. K., & Bunn, S. E. (2012). Temporal and spatial variation in ecosystem metabolism food web carbon transfer in a wet-dry tropical river. *Freshwater Biology*, *57*(3), 435–450. https://doi.org/10.1111/j.1365-2427.2011.02708.x

Huttunen, J. T., Vaisanen, T. S., Hellsten, S. K., Heikkinen, M., Nykanen, H., Jungner, H., et al. (2002). Fluxes of CH_4, CO_2, and N_2O in hydroelectric reservoirs Lokka and Porttipahta in the northern boreal zone in Finland. *Global Biogeochemical Cycles*, *16*(1), 1003. https://doi.org/10.1029/2000GB001316

IPCC (2001). *Climate change 2001: The scientific basis. Intergovernmental Panel on Climate Change*. Cambridge, UK: Cambridge University Press.

Jacinthe, P. A., Filippelli, G. M., Tedesco, L. P., & Raftis, R. (2012). Carbon storage and greenhouse gases emission from a fluvial reservoir in an agricultural landscape. *Catena*, *94*, 53–63. https://doi.org/10.1016/j.catena.2011.03.012

Johnson, M. S., Billet, M. F., Dinsmore, K. J., Walling, M., Dyson, K. E., & Jassal, R. S. (2010). Direct and continuous measurement of dissolved carbon dioxide in freshwater aquatic systems—Method and applications. *Ecohydrology*, *3*, 68–78. https://doi.org/10.1002/eco.95

Junk, W. J., Bayley, P. B., & Sparks, R. E. (1989). The flood pulse concept in river-floodplain systems. *Canadian Special Publication of Fisheries and Aquatic Sciences*, *106*, 110–127.

Kaplan, L. A., & Blott, T. L. (1982). Diel fluctuations of DOC generated by algae in a piedmont stream. *Limnology and Oceanography*, *27*(6), 1091–1100. https://doi.org/10.4319/lo.1982.27.6.1091

Keller, M., & Stallard, R. F. (1994). Methane emission by bubbling from Gatun Lake, Panama. *Journal of Geophysical Research—Atmospheres*, *99*(D4), 8307–8319. https://doi.org/10.1029/92JD02170

Kling, G. W., Kipphut, G. W., & Miller, M. C. (1991). Arctic lakes and streams as gas conduits to the atmosphere: Implications for tundra carbon budgets. *Science*, *251*(4991), 298–301. https://doi.org/10.1126/science.251.4991.298

Kling, G. W., Kipphut, G. W., Miller, M. M., & O'Brien, W. J. (2000). Integration of lakes and streams in a landscape perspective: The importance of material processing on spatial patterns and temporal coherence. *Freshwater Biology*, *43*(3), 477–497. https://doi.org/10.1046/j.1365-2427.2000.00515.x

Knoll, L. B., Vanni, M. J., & Renwick, W. H. (2003). Phytoplankton primary production and photosynthetic parameters in reservoirs along a gradient of watershed land use. *Limnology and Oceanography*, *48*(2), 608–617. https://doi.org/10.4319/lo.2003.48.2.0608

Kone, Y. J. M., Abril, G., Kouadio, K. N., Delille, B., & Borges, A. V. (2009). Seasonal variability of carbon dioxide in the rivers and lagoons of Ivory Coast (West Africa). *Estuaries and Coasts*, *32*(2), 246–260. https://doi.org/10.1007/s12237-008-9121-0

Kutner, M. H., Nachtsheim, C. J., & Neter, J. (2004). *Applied linear regression models*. Boston, Massachusetts: McGraw-Hill Irwin.

Li, B., Xiao, H., Yuan, X., Wilson, J. H. M., Liu, H., Chen, Z., et al. (2013). Analysis of ecological and commercial benefits of a dike-pond project in the drawdown one of the Three Gorges Reservoir. *Ecological Engineering*, *61*, 1–11. https://doi.org/10.1016/j.ecoleng.2013.09.033

Li, S., Bush, R. T., Santos, I. R., Zhang, Q., Song, K., Mao, R., et al. (2018). Large greenhouse gas emissions from China's lakes and reservoirs. *Water Research*, *147*, 13–24. https://doi.org/10.1016/j.watres.2018.09.053

Li, Z., Zhang, Z., Xiao, Y., Guo, J., Wu, S., & Liu, J. (2014). Spatio-temporal variations of carbon dioxide and its gross emission regulated by artificial operation in a typical hydropower reservoir in China. *Environmental Monitoring and Assessment*, *186*, 3023–3039. https://doi.org/10.1007/s10661-013-3598-0

Lofton, D. D., Whalen, S. C., & Hershey, A. E. (2014). Effect of temperature on methane dynamics and evaluation of methane oxidation kinetics in shallow Arctic Alaskan lakes. *Hydrobiologia*, *721*(1), 209–222. https://doi.org/10.1007/s10750-013-1663-x

Lu, f., Yang, L., Wang, X., Duan, X., Mu, Y., Song, W., et al. (2011). Preliminary report on methane emissions from the Three Gorges Reservoir in the summer drainage period. *Journal of Environmental Sciences*, *23*(12), 2029–2033. https://doi.org/10.1016/S1001-0742(10)60668-7

MacIntyre, S., Jonsson, A., Jansson, M., Aberg, J., Turney, D. E., & Miller, S. D. (2010). Buoyancy flux, turbulence, and the gas transfer coefficient in a stratified lake. *Geophysical Research Letters*, *37*, L24604. https://doi.org/10.1029/2010GL044164

Maeck, A., Hofmann, H., & Lorke, A. (2014). Pumping of methane out of aquatic sediments—Ebullition forcing mechanisms in an impounded river. *Biogeosciences*, *11*(11), 2925–2938. https://doi.org/10.5194/bg-11-2925-2014

Mattson, M. D., & Likens, G. E. (1990). Air pressure and methane fluxes. *Nature*, *347*(6295), 718–719. https://doi.org/10.1038/347718b0

McGillis, W. R., Edson, J. B., Zappa, C. J., Ware, J. D., McKenna, S. P., Terray, E. A., et al. (2004). Air-sea CO_2 exchange in the equatorial Pacific. *Journal of Geophysical Research—Oceans*, *109*, C08S02. https://doi.org/10.1029/2003JC002256

McNicol, G., & Silver, W. L. (2014). Separate effects of flooding and anaerobiosis on soil greenhouse gas emissions and redox sensitive biogeochemistry. *Journal of Geophysical Research: Biogeosciences*, *119*, 557–566. https://doi.org/10.1002/2013JG002433

Mendonca, R., Mueller, R. A., Clow, D., Verpooter, C., Raymond, P., Tranvik, L. J., & Sobek, S. (2017). Organic carbon burial in global lakes and reservoirs. *Nature Communications*, *8*(1), 1694. https://doi.org/10.1038/s41467-017-01789-6

Michmerhuizen, C. M., Streigl, R. G., & McDonald, M. E. (1996). Potential methane emission from north-temperate lakes following ice melt. *Limnology and Oceanography*, *41*(5), 985–991. https://doi.org/10.4319/lo.1996.41.5.0985

Myhre, G., Shindell, D., Bréon, F.-M., Collins, W., Fuglestvedt, J., Huang, J., et al. (2013). Anthropogenic and natural radiative forcing. In T. F. Stocker, et al. (Eds.), *Climate change 2013: The physical science basis. Contribution of Working Group I to the Fifth Assessment Report of the Intergovernmental Panel on Climate Change*, (pp. 659–740). Cambridge, U. K., and New York: Cambridge University Press.

Naqvi, S. W. A., Lam, P., Narvenkar, G., Sarkar, A., Naik, H., Pratihary, A., et al. (2018). Methane stimulates massive nitrogen loss from freshwater reservoirs in India. *Nature Communications*, *9*(1), 1265. https://doi.org/10.1038/s41467-018-03607-z

Natchimuthu, S., Sundgren, I., Galfalk, M., Klemedtsson, L., & Bastviken, D. (2017). Spatiotemporal variability of lake pCO_2 and CO_2 fluxes in a hemiboreal catchment. *Journal of Geophysical Research: Biogeosciences*, *122*, 30–49. https://doi.org/10.1002/2016JG003449

Odum, H. T. (1956). Primary production in flowing waters. *Limnology and Oceanography*, *1*(2), 102–117. https://doi.org/10.4319/lo.1956.1.2.0102

Ollivier, Q. R., Maher, D. T., Pitfield, C., &Macreadie, P. I. (2019). Punching above their weight: Large release of greenhouse gases from small agricultural dams. *Global Change Biology*, *25*(2), 721–732. https://doi.org/10.1111/gcb.14477

Ostrovsky, I., McGinnis, D. F., Lapidus, L., & Eckert, W. (2008). Quantifying gas ebullition with echosounder—The role of methane transport by bubbles in a medium-sized lake. *Limnology and Oceanography—Methods*, *6*(2), 105–118. https://doi.org/10.4319/lom.2008.6.105

Peacock, M., Audet, J., Jordan, S., Smeds, J., & Wallin, M. B. (2019). Greenhouse gas emissions from urban ponds driven by nutrient status and hydrology. *Ecosphere*, *10*(3), e02643. https://doi.org/10.1002/ecs2.2643

Peeters, F., Atamanchuk, D., Tengberg, A., Encinas-Fernandez, J., & Hofmann, H. (2016). Lake metabolism—Comparison of lake metabolic rates estimated from a diel CO2 and the common diel O2 technique. *PLOS ONE*, *11*(12), e0168393. https://doi.org/10.1371/journal.pone.0168393

Raymond, P. A., Saiers, J. E., & Sobczak, W. V. (2016). Hydrological and biogeochemical controls on watershed dissolved organic matter transport—Pulse-shunt concept. *Ecology*, *97*(1), 5–16. https://doi.org/10.1890/14-1684.1

Richey, J. E., Devol, A. H., Wofsy, S. C., Victoria, R., & Riberio, M. N. G. (1988). Biogenic gases and the oxidation and reduction of carbon in Amazon River and floodplain waters. *Limnology and Oceanography*, *33*(4.1), 551–561. https://doi.org/10.4319/lo.1988.33.4.0551

Riera, J. L., Schindler, J. E., & Kratz, T. K. (1999). Seasonal dynamics of carbon dioxide and methane in two clear-water lakes and two bog lakes in northern Wisconsin, U.S.A. *Canadian Journal of Fisheries and Aquatic Sciences*, *56*(2), 265–274. https://doi.org/10.1139/f98-182

Sawakuchi, H. O., Bastviken, D., Sawakuchi, A. O., Krusche, A. V., Ballester, M. V. R., & Richey, J. E. (2014). Methane emissions from Amazonian Rivers and their contribution to the global methane budget. *Global Change Biology*, *20*(9), 2829–2840. https://doi.org/10.1111/gcb.12646

Schilder, J. D., Bastviken, D., van Hardenbroek, M., Kankaala, P., Rinta, P., Stotter, T., & Heiri, O. (2013). Spatial heterogeneity and lake morphology affect diffusive greenhouse gas emission estimates of lakes. *Geophysical Research Letters*, *40*, 5752–5756. https://doi.org/10.1002/2013GL057669

Schindler, D. E., Jankowski, K. J., A'Mar, Z. T., & Holtgrieve, G. W. (2017). Two-stage metabolism inferred from diel oxygen dynamics in aquatic ecosystems. *Ecosphere*, *8*(6), e01867. https://doi.org/10.1002/ecs2.1867

Schultz, S., & Conrad, R. (1996). Influence of temperature on pathways to methane production in the permanently cold profundal sediment of Lake Constance. *FEMS Microbiology Ecology*, *20*(1), 1–14. https://doi.org/10.1016/0168-6496(96)00009-8

Segers, R. (1998). Methane production and methane consumption—A review of processes underlying wetland methane fluxes. *Biogeochemistry*, *41*(1), 23–51. https://doi.org/10.1023/A:1005929032764

Smith, K. A., Dobbie, K. E., Ball, B. C., Bakken, L. R., Sitaula, B. K., Hansen, S., et al. (2000). Oxidation of atmospheric methane in Northern European soils, comparison with other ecosystems, and uncertainties in the global terrestrial sink. *Global Change Biology*, *6*(7), 791–803. https://doi.org/10.1046/j.1365-2486.2000.00356.x

St. Louis, V. L., Kelly, C. A., Duchemin, E., Rudd, J. W. M., & Rosenberg, D. M. (2000). Reservoir surface as sources of greenhouse gases to the atmosphere: A global estimate. *BioScience*, *50*(9), 766–775. https://doi.org/10.1641/0006-3568(2000)050[0766:RSASOG]2.0.CO;2

Stets, E. G., Butman, D., McDonald, C. P., Stackpoole, S. M., DeGrandpre, M. D., & Striegl, R. G. (2017). Carbonate buffering and metabolic controls on carbon dioxide in rivers. *Global Biogeochemical Cycles*, *31*, 663–677. https://doi.org/10.1002/2016GB005578

Strayer, R. F., & Tiedje, J. M. (1978). In situ methane production in a small, hypereutrophic hard-water lake: Loss of methane from sediments by vertical diffusion and ebullition. *Limnology and Oceanography*, *23*(6), 1201–1206. https://doi.org/10.4319/lo.1978.23.6.1201

Tobias, C. R., Bohlke, J. K., & Harvey, J. W. (2007). The oxygen-18 isotope approach for measuring aquatic metabolism in high productivity waters. *Limnology and Oceanography—Methods*, *52*(4), 1439–1453. https://doi.org/10.4319/lo.2007.52.4.1439

Tomaszek, J. A., & Czerwieniec, E. (2003). Denitrification and oxygen consumption in bottom sediments: Factors influencing rates of the processes. *Hydrobiologia*, *504*(1-3), 59–65. https://doi.org/10.1023/BB:HYDR.0000008508.81690.10

Vasquez, E., Ejarque, E., Ylla, I., Romaní, A. M., & Butturini, A. (2015). Impact of drying/rewetting cycles on the bioavailability of dissolved organic matter molecular-weight fractions in a Mediterranean stream. *Freshwater Science*, *34*(1), 263–275. https://doi.org/10.1086/679616

Wainright, S. C., Couch, C. A., & Meyer, J. L. (1992). Fluxes of bacteria and organic matter into a blackwater river from river sediments and floodplain soils. *Freshwater Biology*, *28*(1), 37–48. https://doi.org/10.1111/j.1365-2427.1992.tb00560.x

Wang, C., Xiao, S., Li, Y., Zhong, H., Li, X., & Peng, F. (2014). Methane formation and consumption processes in Jiangxi Bay of the Three Gorges Reservoir. *Scientific Reports*, *4*, 4449. https://doi.org/10.1038/srep04449

Wang, Q., Liu, H., Yuan, X., Sun, R., & Wang, J. (2009). Pattern and biodiversity of plant community in water-level-fluctuation zone of Pengxi River after impoundment of the Three Gorges Reservoir. *Journal of Chongqing Normal University—Natural Sciences*, *26*, 48–54.

Wanninkhof, R. (1992). Relationship between wind speed and gas exchange over the ocean. *Journal of Geophysical Research*, *97*(C5), 7373–7382. https://doi.org/10.1029/92JC00188

Wik, M., Thorton, B. F., Bastviken, D., Uhlbaeck, J., & Crill, P. M. (2016). Biased sampling of methane release from northern lakes—A problem for extrapolation. *Geophysical Research Letters*, *43*, 1256–1262. https://doi.org/10.1002/2015GL066501

Wilhelm, E., Battino, R., & Wilcock, R. J. (1977). Low-pressure solubility of gases in liquid water. *Chemical Reviews*, *77*(2), 219–262. https://doi.org/10.1021/cr60306a003

Xiao, S., Liu, D., Wang, Y., Yang, Z., & Chen, W. (2013). Temporal variation of methane flux from Xiangxi Bay of the Three Gorges Reservoir. *Scientific Reports*, *3*(1), 1–8. https://doi.org/10.1038/srep02500

Yang, L., Lu, F., Wang, X., Duan, X., Song, W., Sun, B., et al. (2012). Surface methane emissions from different land use types during various water levels in three major drawdown areas of the Three Gorges Reservoir (2012). *Journal of Geophysical Research*, *117*, D10109. https://doi.org/10.1029/2011JD017362

Yvon-Durocher, G., Allen, A. P., Bastviken, D., Conrad, R., Gudasz, C., St-Pierre, A., et al. (2014). Methane fluxes show consistent temperature dependence across microbial to ecosystem scales. *Nature*, *507*(7493), 488–491. https://doi.org/10.1038/nature13164

Yvon-Durocher, G., Caffrey, J. M., Cescatti, A., Dossena, M., del Giorgio, P., Gasol, J. M., et al. (2012). Reconciling the temperature dependence of respiration across timescales and ecosystem types. *Nature*, *487*(7408), 472–476. https://doi.org/10.1038/nature11205

Zar, J. H. (2010). *Biostatistical analysis*. Upper Saddle River, New Jersey: Pearson.

Zarfl, C., Lumsdon, A. E., Berlekamp, J., Tydecks, L., & Tockner, K. (2015). A global boom in hydropower dam construction. *Aquatic Sciences*, *77*(1), 161–170. https://doi.org/10.1007/s00027-014-0377-0

Zhang, J., Li, S., Dong, R., & Jiang, C. (2018). Physical evolution of the Three Gorges Reservoir using advanced SVM on Landsat images and SRTM DEM data. *Environmental Science and Pollution Research*, *25*(15), 14,911–14,918. https://doi.org/10.1007/s11356-018-1696-9

Zhao, Y., Wu, B. F., & Zeng, Y. (2013). Spatial and temporal patterns of greenhouse gas emissions from Three Gorges Reservoir of China. *Biogeosciences*, *10*(2), 1219–1230. https://doi.org/10.5194/bg-10-1219-2013

Zhou, S., He, Y., Yuan, X., Peng, S., & Yue, J. (2017). Greenhouse gas emissions from different land-use areas in the littoral zone of the Three Gorges reservoir, China. *Ecological Engineering*, *100*, 316–324. https://doi.org/10.1016/jecoleng.2017.01.003

Zhu, D., Chen, H., Yuan, X., Wu, N., Gao, Y., Wu, Y., et al. (2013). Nitrous oxide emissions from the surface of the Three Gorges Reservoir. *Ecological Engineering*, *60*, 150–154. https://doi.org/10.1016/j.ecoleng.2013.07.049

Erratum

In the originally published version of this article, Tables 3, 4, and 5 required corrections to formatting. Additionally, the author contributions were incomplete. The tables and author contributions have since been corrected, and this version may be considered the authoritative version of record.